NCU-HEP-k055
Oct 2012

A Comprehensive Analysis on Lepton Flavor Violating Higgs to $\mu\bar{\tau} + \tau\bar{\mu}$ Decay in Supersymmetry without R Parity

Abdessalem Arhrib*

Department of Mathematics, Faculty of Science and Techniques, B.P 416 Tangier, Morocco.

Yifan Cheng and Otto C. W. Kong†

Department of Physics and Center for Mathematics and Theoretical Physics, National Central University, Chung-li, Taiwan 32054.

In this paper we examine thoroughly Higgs to $\mu\bar{\tau}+\tau\bar{\mu}$ decay via processes involving R-parity violating couplings. By means of full one-loop diagrammatic calculations, we found that even if known experimental constraints, including particularly the stringent sub-eV neutrino mass bounds, giving strong restrictions on some of the R-parity violating parameters, the branching ratio could still achieve notable value in the admissible parameter space. Hence, the flavor violating leptonic decay is of interest to future experiments. We present here key results of our analysis. Based on the analysis, we give some comments on $h^0 \to e\bar{\mu} + \mu\bar{e}$ and $h^0 \to e\bar{\tau} + \tau\bar{e}$ also.

*Electronic address: aarhrib@ictp.it

†Electronic address: otto@phy.ncu.edu.tw

I. INTRODUCTION

As we know, in the Standard Model (SM) lepton number of each flavor is separately conserved. Thus lepton flavor violating (LFV) decays such as Higgs to $\mu\bar{\tau}+\tau\bar{\mu}$ is forbidden. However, neutrino oscillation experiments provide strong evidence that the lepton flavor conservation should be violated [1–4]. If lepton flavor violation can be observed in processes involving only SM particles, this would contribute an important probe to physics beyond the SM. Such processes, in particular the Higgs to $\mu\bar{\tau}+\tau\bar{\mu}$ decay, deserve attention.

Looking into the literature, various sources or scenarios to accommodate LFV interactions have been introduced and analyzed. For examples, adding heavy right-handed neutrinos can give neutrinos mixings and hence lepton flavor violation [5], or a general two Higgs doublet model has LFV interactions due to Yukawa coupling matrices which could not be diagonalized simultaneously [6, 7]. Under the framework of supersymmetry (SUSY), it is well known that nonzero off-diagonal elements of soft SUSY breaking terms in the leptonic sector (A^E, $\tilde{m}_L^2$ and $\tilde{m}_E^2$ – to be precisely defined below) generate LFV couplings. Moreover, the (total) lepton number itself may not conserve. For the SUSY case, such R-parity violating (RPV) couplings also give interesting contributions to processes like Higgs to $\mu\bar{\tau}+\tau\bar{\mu}$.

While SUSY is undoubtedly a popular candidate theory for new physics, its existence is so far in lack of experimental evidence [8]. Thus, some simple versions of supersymmetric model such as constrained minimal supersymmetric standard model, have faced stringent challenges [9]. However, it is pointed out that there are still rooms for (minimal) supersymmetric standard model to accommodate existing experimental constraints [10–13]. For instance, large mass spectrum for the majority of supersymmetric particles around or beyond 1TeV is still to be probed [13]. The heavy spectrum is in accordance with the newly discovered boson mass $\cong$ 125GeV to 126GeV [14–16]. A large portion of the parameter space remains uncovered in versions of the minimal supersymmetric standard model (MSSM) with more free parameters [11]. Non-universality of soft SUSY breaking masses is also a possible explanation to the non-observation of supersymmetric signals [12].

Under the scheme of the MSSM, various LFV decays such as $\tau\to\mu\gamma$, $\tau\to\mu X$, $\tau\to\mu\eta$, $\tau\to\mu\mu\mu$, and so on [17], as well as Higgs to $\mu\bar{\tau}+\tau\bar{\mu}$ decay [7, 18] which we put our focus on in this paper, have been discussed. However, in many studies of the MSSM, R parity is often imposed by hand to prevent proton decay and make the lightest supersymmetric particle a

possible dark matter candidate. From the theoretical point of view, R parity is *ad hoc* and not well motivated so long as the phenomenological (minimal) supersymmetric standard model is concerned [19]. A generic supersymmetric standard model (without R parity imposed), on the contrary, not only provides a convenient way to lepton flavor violation, but also has the advantage of a richer phenomenology including neutrino masses and mixings without introducing any extra superfield. Under the framework of SUSY with R parity violation, there have been some studies [20, 21] on the issue of lepton flavor violation. Nevertheless, such studies were either limited to particular types of R-parity violation or did not take $h^0 \to \mu\bar{\tau} + \tau\bar{\mu}$ into consideration. While recently both ATLAS and CMS [14, 15] reported discovery of a boson state which is essentially compatible with a SM-like Higgs, more data is needed to pin down its nature and the flavor violating Higgs decay such as $h^0 \to \mu\bar{\tau} + \tau\bar{\mu}$ is especially interesting at this moment. In this paper, we will investigate thoroughly LFV Higgs to $\mu\bar{\tau} + \tau\bar{\mu}$ decay from SUSY without R parity via full diagrammatic calculations up to one-loop level. Best branching ratios for the decay from various RPV parameter combinations, under a reasonable choice of an experimentally viable region of the background parameter space, will be reported. Note that a part of key results has been reported, with limited presentation of analytical expressions and discussions, in a short letter [22].

In following section, we summarize our basic formulation and parameterization of the generic supersymmetric standard model (without R parity). Particularly, the neutral and charged Higgs mass terms, including loop corrections (up to two-loop for neutral Higgs case), would be discussed. Then we give a sketch of our calculations and show numerical results from all possible RPV parameter combinations in section 3. Note that during our analysis we made no assumptions on the RPV parameters. The mass spectrum of all SUSY particles as well as the Higgs boson are kept within experimental constraints. Finally, we conclude this paper with some remarks in section 4. Lists of all one-loop diagrams and useful effective couplings would be given in appendices in the last. We may be including more details than necessary, particularly in the sense of showing some experimentally uninteresting results. We include those to give a full picture about the physics involved, so that readers can appreciate the key features leading to the interesting or uninteresting results. Some of the lessons one can learn from the analysis would be useful for future studies of other related aspects of the model. Under the same consideration, we give detailed expressions of the couplings involved and the Feynman diagrams in the appendices.

II. ON THE SUPERSYMMETRIC STANDARD MODEL WITHOUT R PARITY AND THE SCALAR MASS MATRICES

A. Formulation and parameterization

With content of minimal superfields spectrum, the most general renormalizable superpotential without R parity can be written as

$$W = \epsilon_{ab}\left[\mu_\alpha \hat{H}_u^a \hat{L}_\alpha^b + h_{ik}^u \hat{Q}_i^a \hat{H}_u^b \hat{U}_k^C + \lambda'_{\alpha jk}\hat{L}_\alpha^a \hat{Q}_j^b \hat{D}_k^C + \frac{1}{2}\lambda_{\alpha\beta k}\hat{L}_\alpha^a \hat{L}_\beta^b \hat{E}_k^C\right] + \frac{1}{2}\lambda''_{ijk}\hat{U}_i^C \hat{D}_j^C \hat{D}_k^C \quad (1)$$

where (a, b) are SU(2) indices with $\epsilon_{12} = -\epsilon_{21} = 1$, (i, j, k) are the usual family (flavor) indices, and (α, β) are extended flavor indices going from 0 to 3. Note that λ is antisymmetric in the first two indices as required by SU(2) product rules while λ'' is antisymmetric in the last two indices by $\mathrm{SU}(3)_C$. The soft SUSY breaking terms can be written as follows:

$$\begin{aligned} V_{\rm soft} =& \epsilon_{ab} B_\alpha\, H_u^a \tilde{L}_\alpha^b + \epsilon_{ab}\left[A_{ij}^U \tilde{Q}_i^a H_u^b \tilde{U}_j^C + A_{ij}^D H_d^a \tilde{Q}_i^b \tilde{D}_j^C + A_{ij}^E H_d^a \tilde{L}_i^b \tilde{E}_j^C\right] + \text{h.c.} \\ &+ \epsilon_{ab}\left[A_{ijk}^{\lambda'} \tilde{L}_i^a \tilde{Q}_j^b \tilde{D}_k^C + \frac{1}{2}A_{ijk}^{\lambda} \tilde{L}_i^a \tilde{L}_j^b \tilde{E}_k^C\right] + \frac{1}{2}A_{ijk}^{\lambda''} \tilde{U}_i^C \tilde{D}_j^C \tilde{D}_k^C + \text{h.c.} \\ &+ \tilde{Q}^\dagger \tilde{m}_Q^2 \tilde{Q} + \tilde{U}^\dagger \tilde{m}_U^2 \tilde{U} + \tilde{D}^\dagger \tilde{m}_D^2 \tilde{D} + \tilde{L}^\dagger \tilde{m}_L^2 \tilde{L} + \tilde{E}^\dagger \tilde{m}_E^2 \tilde{E} + \tilde{m}_{H_u}^2 |H_u|^2 \\ &+ \frac{M_1}{2}\tilde{B}\tilde{B} + \frac{M_2}{2}\tilde{W}\tilde{W} + \frac{M_3}{2}\tilde{g}\tilde{g} + \text{h.c.}\,, \end{aligned} \quad (2)$$

where $\tilde{L}^\dagger \tilde{m}_{\tilde{L}}^2 \tilde{L}$ is given by a 4×4 matrix. $\tilde{m}_{L_{00}}^2$ corresponds to $\tilde{m}_{H_d}^2$ in MSSM, while $\tilde{m}_{L_{0k}}^2$'s give new mass mixings.

The above, together with the standard (gauged) kinetic terms, describe the full Lagrangian of the model. We have four $\hat{L}$ superfields, which contain the components of fermion doublet as l^0 and l^-, while their scalar partners as $\tilde{l}^0$ and $\tilde{l}^-$. In principle, the neutral scalar part $\tilde{l}_\alpha^0$ of all four $\hat{L}$ superfields can bear vacuum expectation values (VEV). To make the analysis simple and physics more transparent, we use a parameterization which picks a basis such that the direction of VEV is singled out, i.e. only $\hat{L}_0$ bears a nonzero VEV among four $\hat{L}$'s. This procedure guarantee $\hat{L}_0$ can be always identified as $\hat{H}_d$ in MSSM. The two superfields have the same quantum number as the symmetry of lepton number which makes the distinction between $\hat{L}$ and $\hat{H}_d$ as by definition not part of the model. However, one should keep in mind that $\hat{H}_d$ may contain partly the charged lepton states. It is also worth mentioning here that the down quark and charged lepton Yukawa coupling matrix are both diagonal under our parameterization while up quark Yukawa coupling is the product of CKM

factors and diagonal quark masses. The parameterization has the advantage that tree level RPV contributions to fermion mass matrices are described completely by the μ_i, B_i, and $\tilde{m}^2_{L_{0i}}$ parameters, which are well constrained to be small even with just very conservative neutrino mass bounds imposed [23, 24].

Now we turn to the issue about mass matrices of matter fields. In our framwork, the three known charged leptons, together with two charginos, correspond to the mass eigenstates of a 5×5 charged fermion matrix $\mathcal{M}_C$, which can be diagonalized by two unitary matrices as $\boldsymbol{V}^\dagger \mathcal{M}_C \boldsymbol{U} = \mathrm{diag}\left\{M_{\chi_n^-}\right\} \equiv \mathrm{diag}\left\{M_{c1}, M_{c2}, m_e, m_\mu, m_\tau\right\}$. For neutral fermions, we take four heavy neutralinos and three very light neutrinos as mass eigenstates under the scheme of a 7×7 neutral fermion mass matrix $\mathcal{M}_\mathcal{N}$. By using a unitary matrix $\boldsymbol{X}$, the diagonalization can be done as $\boldsymbol{X}^T \mathcal{M}_\mathcal{N} \boldsymbol{X} = \mathrm{diag}\left\{M_{\chi_n^0}\right\} \equiv \mathrm{diag}\left\{M_{n_{i=1,4}}, m_{\nu_1}, m_{\nu_2}, m_{\nu_3}\right\}$. On considering the squark sectors, the up-squark mass-squared matrix looks exactly the same as the one in MSSM, while down-squark one contains new contribution from RPV terms. They can be diagonalized separately as $\mathcal{D}^{u\dagger} \mathcal{M}^2_U \mathcal{D}^u = \mathrm{diag}\{\mathcal{M}^2_{\mathrm{U}}\}$ and $\mathcal{D}^{d\dagger} \mathcal{M}^2_D \mathcal{D}^d = \mathrm{diag}\{\mathcal{M}^2_{\mathrm{D}}\}$. All the mass matrices mentioned above can be found in [23].

B. Scalar mass matrices and loop corrections

For neutral scalar mass matrix, we have now five neutral complex scalar fields from $\hat{H}_u$ and four $\hat{L}_\alpha$'s. Explicitly, we write the $(1+4)$ complex fields in terms of their scalar and pseudoscalar parts, in the order $\{h_u^{0\dagger}, \tilde{l}_0^0, \tilde{l}_1^0, \tilde{l}_2^0, \tilde{l}_3^0\}$ to form a full 10×10 (real and symmetric) mass-squared matrix, which (in tree-level) can be written as

$$\mathcal{M}^2_S = \begin{pmatrix} \mathcal{M}^2_{SS} & \mathcal{M}^2_{SP} \\ (\mathcal{M}^2_{SP})^T & \mathcal{M}^2_{PP} \end{pmatrix} , \tag{3}$$

where the scalar, pseudoscalar, and mixing parts are

$$\begin{aligned} \mathcal{M}^2_{SS} &= \mathrm{Re}(\mathcal{M}^2_\phi) + 2\,\mathcal{M}^2_{\phi\phi} , \\ \mathcal{M}^2_{PP} &= \mathrm{Re}(\mathcal{M}^2_\phi) , \\ \mathcal{M}^2_{SP} &= -\mathrm{Im}(\mathcal{M}^2_\phi) , \end{aligned} \tag{4}$$

respectively, with

$$\mathcal{M}^2_{\phi\phi} = \frac{1}{2}\, M_Z^2 \begin{pmatrix} \sin^2\beta & -\cos\beta\,\sin\beta & 0_{1\times 3} \\ -\cos\beta\,\sin\beta & \cos^2\beta & 0_{1\times 3} \\ 0_{3\times 1} & 0_{3\times 1} & 0_{3\times 3} \end{pmatrix} , \tag{5}$$

and

$$\mathcal{M}^2_{\phi} = \begin{pmatrix} \tilde{m}^2_{H_u} + \mu^*_\alpha\mu_\alpha + M_Z^2\,\cos 2\beta\,\left[-\frac{1}{2}\right] & -(B_\alpha) \\ -(B^*_\alpha) & \tilde{m}^2_L + (\mu^*_\alpha\mu_\beta) + M_Z^2\,\cos 2\beta\,\left[\frac{1}{2}\right] I_{4\times 4} \end{pmatrix} . \tag{6}$$

As for charged (colorless) scalars, we should treat charged Higgs and sleptons on an equal footing. The basis $\{h_u^{+\dagger}, \tilde{l}_0^-, \tilde{l}_1^-, \tilde{l}_2^-, \tilde{l}_3^-, \tilde{l}_1^{+\dagger}, \tilde{l}_2^{+\dagger}, \tilde{l}_3^{+\dagger}\}$ as $1+4+3$ form from $\hat{H}_u$, four $\hat{L}_\alpha$'s and three $\hat{E}_i^C$'s is used to write the 8×8 charged scalar mass-squared matrix, which can be written as

$$\mathcal{M}^2_E = \begin{pmatrix} \widetilde{\mathcal{M}}^2_{H_u} & \widetilde{\mathcal{M}}^{2\dagger}_{LH} & \widetilde{\mathcal{M}}^{2\dagger}_{RH} \\ \widetilde{\mathcal{M}}^2_{LH} & \widetilde{\mathcal{M}}^2_{LL} & \widetilde{\mathcal{M}}^{2\dagger}_{RL} \\ \widetilde{\mathcal{M}}^2_{RH} & \widetilde{\mathcal{M}}^2_{RL} & \widetilde{\mathcal{M}}^2_{RR} \end{pmatrix} , \tag{7}$$

where

$$\begin{aligned} \widetilde{\mathcal{M}}^2_{H_u} &= \tilde{m}^2_{H_u} + \mu^*_\alpha\mu_\alpha + M_Z^2\,\cos 2\beta\left[\frac{1}{2} - \sin^2\theta_W\right] \\ &\quad + M_Z^2\,\sin^2\beta\,[1-\sin^2\theta_W] , \\ \widetilde{\mathcal{M}}^2_{LL} &= \tilde{m}^2_L + m_L^\dagger m_L + (\mu^*_\alpha\mu_\beta) + M_Z^2\,\cos 2\beta\left[-\frac{1}{2} + \sin^2\theta_W\right] I_{4\times 4} \\ &\quad + \begin{pmatrix} M_Z^2\,\cos^2\beta\,[1-\sin^2\theta_W] & 0_{1\times 3} \\ 0_{3\times 1} & 0_{3\times 3} \end{pmatrix} , \\ \widetilde{\mathcal{M}}^2_{RR} &= \tilde{m}^2_E + m_E m_E^\dagger + M_Z^2\,\cos 2\beta\left[-\sin^2\theta_W\right] I_{3\times 3} , \end{aligned} \tag{8}$$

and

$$\begin{aligned} \widetilde{\mathcal{M}}^2_{LH} &= (B^*_\alpha) + \begin{pmatrix} \frac{1}{2}\,M_Z^2\,\sin 2\beta\,[1-\sin^2\theta_W] \\ 0_{3\times 1} \end{pmatrix} , \\ \widetilde{\mathcal{M}}^2_{RH} &= -(\,\mu_i^*\lambda_{i0k}\,)\,\frac{v_0}{\sqrt{2}} = (\,\mu_k^*\,m_k\,) \qquad \text{(no sum over } k) \quad , \\ (\widetilde{\mathcal{M}}^2_{RL})^T &= \begin{pmatrix} 0 \\ A^E \end{pmatrix} \frac{v_0}{\sqrt{2}} - (\,\mu^*_\alpha\lambda_{\alpha\beta k}\,)\,\frac{v_u}{\sqrt{2}} , \end{aligned} \tag{9}$$

with $m_L = \mathrm{diag}\{0, m_E\} = \mathrm{diag}\{0, m_1, m_2, m_3\}$. m_i's ($\approx m_{e_i}$ under small-μ_i scenario) are mass parameters in charged fermion mass matrix [23]. Furthermore, the two scalar mass-squared matrices can be diagonalized as $\mathcal{D}^{s\,T}\mathcal{M}_S^2\mathcal{D}^s = \mathrm{diag}\{M^2_{S\,m=1,10}\}$ and $\mathcal{D}^{l\,\dagger}\mathcal{M}_E^2\mathcal{D}^l = \mathrm{diag}\{M^2_{\tilde{\ell}_{n=1,8}}\}$, which will become useful later.

Different from MSSM, the physical scalar states are now mixture of Higgses and sleptons. The RPV terms provide new contribution to scalar mass matrices and hence Higgs mass. In addition, radiative corrections, especially those from third generation quarks and squarks, could play important roles in Higgs mass. Accordingly, we implement complete one-loop corrections [25] to matrix elements directly relating to Higgs bosons (CP-even, CP-odd and charged ones as well) during our computation. Moreover, light Higgs mass should be treated delicately because of the newly discovered boson mass $\cong$ 125GeV to 126GeV by Large Hadron Collider (LHC) [14, 15]. Therefore we include further an estimation [26] of key two-loop corrections in light Higgs related elements[1]. Note that radiative RPV corrections are typically too small to be taken into account, thus we study tree level RPV effects only.

Under the scheme of MSSM without R parity, the one-loop effective Higgs potential is (recall that $\hat{H}_d \equiv \hat{L}_0$ after our parameterization being chosen):

$$\begin{aligned} V_{\text{eff}} = & \left(\tilde{m}^2_{H_u} + |\mu_\alpha|^2\right)|H_u|^2 + \left(\tilde{m}^2_{L_{00}} + |\mu_0|^2\right)|H_d|^2 + \left(\epsilon_{ab}B_0 H_u^a H_d^b + \text{h.c.}\right) \\ & + \frac{1}{8}\left(g_2^2 + g'^2\right)|H_u|^4 + \frac{1}{8}\left(g_2^2 + g'^2\right)|H_d|^4 + \frac{1}{4}\left(g_2^2 - g'^2\right)|H_u|^2\,|H_d|^2 - \frac{1}{2}g_2^2\left|\epsilon_{ab}H_u^a H_d^b\right|^2 \\ & + \frac{3}{32\pi^2}\sum_{q=t,b}\left[\sum_{i=1,2}\tilde{m}^4_{q_i}\left(\ln\frac{\tilde{m}^2_{q_i}}{Q^2} - \frac{3}{2}\right) - 2\bar{m}_q^4\left(\ln\frac{\bar{m}_q^2}{Q^2} - \frac{3}{2}\right)\right], \end{aligned} \tag{10}$$

where Q is the renormalization scale which should be around weak scale (10^2 to 10^3 GeV). $\tilde{m}^2_{q_i}$ and $\bar{m}^2_q$ denote (Higgs background fields-dependent) eigenvalues of the squark and quark mass matrices respectively.

By using following linear expansion of Higgs bosons (with a relative complex phase for generality),

$$H_u = \begin{pmatrix} h_u^+ \\ \frac{1}{\sqrt{2}}\left(v_u + h_u^s - i h_u^a\right) \end{pmatrix}, \qquad H_d = e^{i\theta_v}\begin{pmatrix} \frac{1}{\sqrt{2}}\left(v_d + h_d^s + i h_d^a\right) \\ h_d^- \end{pmatrix}, \tag{11}$$

[1] Though the Higgs bosons mix with the sleptons via RPV terms, we can still identify the Higgs bosons out of other sleptons due to the foreseeable smallness of RPV parameters.

tadpole equations can be written as

$$
\begin{aligned}
v_d \mathrm{Re}(B_0 e^{i\theta_v}) &= \left(\tilde{m}^2_{H_u} + |\mu_\alpha|^2\right) v_u + \frac{1}{8}\left(g_2^2 + g'^2\right) v_u \left(v_u^2 - v_d^2\right) \\
&\quad + \frac{3}{16\pi^2}\left[\sum_{q=t,b}\sum_{i=1,2} m^2_{\tilde{q}_i} \left\langle \frac{\partial \tilde{m}^2_{q_i}}{\partial h^s_u}\right\rangle \left(\ln\frac{m^2_{\tilde{q}_i}}{Q^2} - 1\right) - 2m_t^2 \left\langle \frac{\partial \bar{m}^2_t}{\partial h^s_u}\right\rangle \left(\ln\frac{m_t^2}{Q^2} - 1\right)\right] \\
v_u \mathrm{Re}(B_0 e^{i\theta_v}) &= \left(\tilde{m}^2_{L_{00}} + |\mu_0|^2\right) v_d + \frac{1}{8}\left(g_2^2 + g'^2\right) v_d \left(v_d^2 - v_u^2\right) \\
&\quad + \frac{3}{16\pi^2}\left[\sum_{q=t,b}\sum_{i=1,2} m^2_{\tilde{q}_i} \left\langle \frac{\partial \tilde{m}^2_{q_i}}{\partial h^s_d}\right\rangle \left(\ln\frac{m^2_{\tilde{q}_i}}{Q^2} - 1\right) - 2m_b^2 \left\langle \frac{\partial \bar{m}^2_b}{\partial h^s_d}\right\rangle \left(\ln\frac{m_b^2}{Q^2} - 1\right)\right] \\
v_{d(u)} \mathrm{Im}(B_0 e^{i\theta_v}) &= +(-)\frac{3}{16\pi^2}\sum_{q=t,b}\sum_{i=1,2} m^2_{\tilde{q}_i} \left\langle \frac{\partial \tilde{m}^2_{q_i}}{\partial h^a_{u(d)}}\right\rangle \left(\ln\frac{m^2_{\tilde{q}_i}}{Q^2} - 1\right) ,
\end{aligned} \tag{12}
$$

where $m^2_{\tilde{q}_i} = \left\langle \tilde{m}^2_{q_i}\right\rangle$ is the squark mass-squared, while expressions for the derivatives with respect to the scalar fields in the bracket (including second derivatives used later) are complicated so we do not list here. One can see, [25] for example, for details[2].

Tadpole equations along the direction of other scalars/sleptons can be obtained easily from scalar potential terms which are related to neutral sleptons[3]:

$$
\begin{aligned}
V = \sum_{i,j=1,3} \Big[& \left(\tilde{m}^2_{L_{ij}} + \mu_i^* \mu_j\right) \tilde{l}_i^{0*} \tilde{l}_j^0 + \left(\tilde{m}^2_{L_{i0}} + \mu_0 \mu_i^*\right) h_d^0 \tilde{l}_i^{0*} + \left(\tilde{m}^2_{L_{0i}} + \mu_0^* \mu_i\right) h_d^{0*} \tilde{l}_i^0 \\
& + \frac{1}{8}\left(g_2^2 + g'^2\right)\left(\left|\tilde{l}_i^0\right|^2 \left|\tilde{l}_j^0\right|^2 - 2\left|\tilde{l}_i^0\right|^2 \left|h_u^0\right|^2 + 2\left|\tilde{l}_i^0\right|^2 \left|h_d^0\right|^2\right) - \left(B_i h_u^0 \tilde{l}_i^0 + \mathrm{h.c.}\right) \Big] ,
\end{aligned} \tag{13}
$$

while vanishing derivatives of V give

$$
B_i \tan\beta = \tilde{m}^2_{L_{0i}} + \mu_0^* \mu_i \, . \tag{14}
$$

The exact form of tree level elements of scalar matrices are as mentioned above, while the one-loop corrections from third generation quarks and squarks are:

$$
\begin{aligned}
\mathcal{M}^{\mathrm{Loop}}_{jk} = \frac{3}{16\pi^2}\sum_{q=t,b}\Big\{ & \sum_{i=1,2}\left[\left\langle \frac{\partial \tilde{m}^2_{q_i}}{\partial \phi_j}\right\rangle \left\langle \frac{\partial \tilde{m}^2_{q_i}}{\partial \phi_k}\right\rangle \ln\frac{m^2_{\tilde{q}_i}}{Q^2} + m^2_{\tilde{q}_i}\left\langle \frac{\partial^2 \tilde{m}^2_{q_i}}{\partial \phi_j \partial \phi_k}\right\rangle \left(\ln\frac{m^2_{\tilde{q}_i}}{Q^2} - 1\right)\right] \\
& - 2\left[\left\langle \frac{\partial \bar{m}^2_q}{\partial \phi_j}\right\rangle \left\langle \frac{\partial \bar{m}^2_q}{\partial \phi_k}\right\rangle \ln\frac{m_q^2}{Q^2} + m_q^2 \left\langle \frac{\partial^2 \bar{m}^2_q}{\partial \phi_j \partial \phi_k}\right\rangle \left(\ln\frac{m_q^2}{Q^2} - 1\right)\right] \Big\} .
\end{aligned} \tag{15}
$$

[2] There may be sign difference between the expression for derivatives in the reference and ours due to definition of linear expansion of scalars.

[3] Conceptually, $\tilde{l}_i^0$ is not the usual $\tilde{\nu}_i$ since l_i^0 deviates from ν_i slightly, with parameter μ_i characterizing the deviation between them. See [23] for details.

In the case of neutral scalars, j and k can be any number among $1, 2, 6, 7$ which is corresponding to h_u^s, h_d^s, h_u^a and h_d^a respectively. As to charged scalar case, j and k can only take the value of 1 or 2, with $\phi_j = \{h_u^+, h_d^+\}$ and $\phi_k = \{h_u^-, h_d^-\}$. With the one-loop corrections and the estimation of two-loop corrections [26] added to the mass terms, we can make sure the Higgs mass generated by our program being with enough accuracy.

III. CALCULATIONS AND NUMERICAL RESULTS

At tree level, neutral Higgs can decay into $\mu\bar{\tau}$ or $\tau\bar{\mu}$ directly via RPV neutral scalar-charged lepton-charged lepton coupling which is absent in MSSM. Otherwise, it can decay through one-loop diagrams (or higher loop diagrams). We list in appendix A all possible one-loop diagrams containing RPV couplings for a neutral scalar decaying to $\mu\bar{\tau}$ while RPV effective couplings we used among all relevant mass eigenstates are listed in appendix B. In our numerical computation, we put all the tree level mass matrices into program and deal directly with mass eigenstates which is obtained by diagonalizing corresponding mass matrix numerically. The one-loop and two-loop corrections as mentioned in section 2 to matrix elements which is most relevant to Higgs mass are also implemented. To make analysis representative enough, we have fully calculated all the (tree and one-loop) diagrams that may contribute. By encoding the analytical formulas of decay amplitude into program, and using *LoopTools* [27] program for the evaluation of loop functions, the numerical value of total amplitude and hence decay rate can be obtained. With total width being the RPV decay rate of $h^0 \to \mu\bar{\tau} + \tau\bar{\mu}$ we got, plus MSSM one which is obtained by including all the widths of significant decay channel such as $\bar{b}b$, $\tau^-\tau^+$, WW^*, ZZ^*, $\gamma\gamma$, and gg, we have the branching ratio of $h^0 \to \mu\bar{\tau} + \tau\bar{\mu}$.

Our aim is to use a concrete setting that is compatible with known constraints but not otherwise too restrictive, to illustrate what we expect to be more generic features of the RPV signature. During numerical analysis, following restrictions and assumptions are used: $|\mu_0|$, $|A_u|$, $|A_d|$ and $\left|A^\lambda\right| \leq 2500\text{GeV}$; A_e is set to be zero since its influence is quite small and negligible; $\tilde{m}_E^2 = \tilde{m}_L^2$ (without zeroth component) $\leq (2500\text{GeV})^2$ with off-diagonal elements zero; $\tan\beta$ ranges from 3 to 60; heavy Higgs/sneutrino and charged Higgs/slepton masses are demanded to be between 200GeV to 3TeV. Furthermore, after considering the uncertainties in experimental Higgs mass and loop corrections to Higgs

mass terms, we kept numerical light Higgs mass to be in the range of 123 to 127GeV. We adopt the relation $M_2 = \frac{1}{3.5}M_3 = 2M_1$ between three gaugino masses and the condition that squarks of the first two families cannot be lighter than about $0.8M_3$. Therefore we take soft SUSY breaking scalar masses $\tilde{m}_Q^2 = \tilde{m}_U^2 = \tilde{m}_D^2 = (0.8M_3 \times \text{identity matrix})^2$ for simplicity and $M_2 \leq 2500$GeV in our analysis. The parameter setting is in accordance with the gravity-mediated SUSY breaking picture [28], for instance.

There are several different sources which can give constraints on our RPV parameter setting. Among which, the one from indirect evidence of neutrino mass, i.e. $\sum_i m_{\nu_i} \lesssim 1$eV [29] is quite crucial. However, since it has not been completely ruled out for neutrinos having mass larger than 1eV, we give some comments on branching ratios as references under the condition that neutrino mass constrained only by the solid bounds, i.e. $m_{\nu_e} < 3$eV, $m_{\nu_\mu} <$ 190KeV and $m_{\nu_\tau} < 18.2$MeV [30] as well. Besides, to prevent B_i from being unreasonably large, we set by hand 1% of B_0 as upper bound in the circumstance of extraordinary loose or no available experimental bounds. Note that all LFV couplings/mass mixings that conserve R parity have been turned off during our analysis. That is to single out the effects of the RPV ones. The reported numerical branching ratios are the best numbers we found under the framework.

A. Contribution from $B_i\,B_j$ combinations

The constraints on this type of combinations are mainly from neutrino mass experiments. The RPV parameter B_i can give contributions to neutrino masses via one-loop diagrams [31]. Generally speaking, larger sneutrino and neutralino masses will raise the upper bound of B_i.

Except for the combinations B_2B_3 and B_1B_1, B_iB_j combinations can only give contributions to the decay from the Type2No.4 diagram (in Appendix A). Since heavy charged scalar masses will severely suppress this diagram, we can have relatively larger amplitudes only in the existence of light charged scalar(s). For the B_2B_3 combination many diagrams contribute, hence its behavior is quite complicated. Basically, the decay amplitude from B_2B_3 tends to increase when soft SUSY breaking scalar masses and gaugino masses get heavier due to the rise of the upper bound on B_i from neutrino masses as mentioned above. Note that B_2 or B_3 alone can give contributions to the $h^0 \to \mu\bar{\tau} + \tau\bar{\mu}$ decay as well. Such contributions are, unavoidably, included in all combinations containing B_2 or B_3. Combina-

tions that are not listed give zero contribution at one-loop level. Similar for the other kinds of RPV parameter combinations given below. Our results are shown in Table 1.

Table 1. $B_i\, B_j$ contributions to branching ratio of $h^0 \to \mu\bar{\tau} + \tau\bar{\mu}$

RPV Parameter Combinations	With Neutrino Mass $\lesssim$1eV Constraint	With Relaxed Neutrino Mass Constraint
$B_1\, B_2$	4×10^{-22}	3×10^{-21}
$B_1\, B_3$	3×10^{-22}	3×10^{-21}
$B_2\, B_2$	9×10^{-23}	4×10^{-15}
$B_2\, B_3$	2×10^{-11}	3×10^{-10}
$B_3\, B_3$	8×10^{-23}	4×10^{-16}

B. Contribution from $B_i\, \mu_j$ combinations

The $B_i\, \mu_j$ type of combinations gets constrained from several sources. The values of B_i and $B_i\mu_j$ are highly constrained separately by their loop contribution to neutrino masses [31]. On the other hand, a non-zero μ_j will induce tree level neutrino mass, hence it is also constrained. The non-observation of leptonic radiative decays like $\mu \to e\gamma$, etc. also give upper bounds on $B_i\mu_j$, say, $|B_1^*\mu_3|$, $|B_2^*\mu_3|$, $|B_3\mu_1^*|$ and $|B_3\mu_2^*| \lessapprox 10^{-4}\,|\mu_0|^3$; $|B_1^*\mu_2|$ and $|B_2\mu_1^*| \lessapprox 7 \times 10^{-7}\,|\mu_0|^3$ [21].

All $B_i\mu_j$ combinations except $B_2\mu_3$ and $B_3\mu_2$ can give contribution to the Higgs decay only from the Type2No.4 diagram. Again light charged scalars preferred for the case. However, these contributions (from the Type2No.4 diagram) can not provide a significant branching ratio. Hence we have the uninterestingly tiny numbers as shown in Table 2.

As for $B_2\mu_3$ and $B_3\mu_2$, both give contributions to the Higgs decay from several diagrams. Among them, the tree diagram [22] is the most important one over a wide range of parameter space. Especially, for the $B_3\mu_2$ combination, a key contribution to the decay amplitude is enhanced by the tau Yukawa coupling y_{e_3} via a term proportional to

$$y_{e_3} M_2^* B_3 \mu_2^* / \left[(\mu_0 M_2 - M_W^2 \sin 2\beta) M_s^2\right]$$

(M_s^2 denotes a generic real scalar mass eigenvalue). The later makes the branching ratio from $B_3\mu_2$ the largest one among all $B_i\mu_j$'s. There is a similar feature for the contributions

from the $B_2\mu_3$ combination, but with a muon Yukawa y_{e_2} instead. These two combinations get their best values under small μ_0 and M_s^2 as can be seen from the expression above.

Table 2. $B_i\,\mu_j$ contributions to branching ratio of $h^0 \to \mu\bar{\tau} + \tau\bar{\mu}$

RPV Parameter Combinations	With Neutrino Mass $\lesssim$1eV Constraint	With Relaxed Neutrino Mass Constraint
$B_1\,\mu_2$	1×10^{-24}	6×10^{-22}
$B_1\,\mu_3$	1×10^{-24}	6×10^{-22}
$B_2\,\mu_1$	9×10^{-23}	8×10^{-22}
$B_2\,\mu_2$	4×10^{-26}	6×10^{-15}
$B_2\,\mu_3$	1×10^{-15}	9×10^{-6}
$B_3\,\mu_1$	8×10^{-23}	7×10^{-22}
$B_3\,\mu_2$	1×10^{-13}	7×10^{-4}
$B_3\,\mu_3$	4×10^{-26}	4×10^{-16}

If we allow neutrino masses being larger than 1eV while making μ_0 large enough to unfasten restrictions by leptonic radiative decays, the main constraint will be from $B_i\mu_j$ loop contribution to neutrino masses. Specifically, by demanding $B_2\mu_3$ and $B_3\mu_2$ contribution to neutrino masses to be just smaller than 190keV, their corresponding branching ratios increase significantly to the order of 10^{-6} and 10^{-4}. Note that as in B_iB_j case, contributions from B_2 and B_3 alone are included.

In fact, analyses similar to the above can be applied to $h^0 \to e\bar{\mu} + \mu\bar{e}$ and $h^0 \to e\bar{\tau} + \tau\bar{e}$ as well. The $B_i\mu_j$ contributions to $h^0 \to e\bar{\mu} + \mu\bar{e}$ is expected to be tiny due to the smallness of the corresponding Yukawa couplings y_{e_1} and y_{e_2}. On the other hand, while the contributions from $B_1\mu_3$ is also suppressed by a relative factor of y_{e_1}/y_{e_2}, and the contributions from $B_3\mu_1$ to $h^0 \to e\bar{\tau} + \tau\bar{e}$ could be roughly the same order as that of $h^0 \to \mu\bar{\tau} + \tau\bar{\mu}$. Hence, the $h^0 \to e\bar{\tau} + \tau\bar{e}$ decay may also be of interest.

C. Contribution from $B_i\,\lambda$ combinations

Apart from the constraint on the B_i parameters, the λ type parameters are bounded by charged current experiments [32]. Generally speaking, increasing soft SUSY breaking slepton masses and gaugino masses leads to heavier chraged slepton, sneutrino and neutralino masses hence raises the upper bounds for B_i and λ.

Table 3. $B_i\,\lambda$ contributions to branching ratio of $h^0 \to \mu\bar{\tau} + \tau\bar{\mu}$

RPV Parameter Combinations	With Neutrino Mass $\lesssim$1eV Constraint	With Relaxed Neutrino Mass Constraint
$B_1\,\lambda_{123}$	1×10^{-5}	4×10^{-5}
$B_1\,\lambda_{132}$	3×10^{-5}	7×10^{-5}
$B_1\,\lambda_{232}$	4×10^{-22}	1×10^{-21}
$B_1\,\lambda_{233}$	5×10^{-25}	2×10^{-24}
$B_2\,\lambda_{123}$	7×10^{-23}	5×10^{-15}
$B_2\,\lambda_{131}$	9×10^{-24}	5×10^{-15}
$B_2\,\lambda_{132}$	5×10^{-22}	5×10^{-15}
$B_2\,\lambda_{232}$	3×10^{-5}	6×10^{-2}
$B_2\,\lambda_{233}$	7×10^{-23}	5×10^{-15}
$B_3\,\lambda_{121}$	5×10^{-24}	4×10^{-16}
$B_3\,\lambda_{123}$	7×10^{-23}	4×10^{-16}
$B_3\,\lambda_{132}$	5×10^{-22}	1×10^{-17}
$B_3\,\lambda_{232}$	5×10^{-22}	4×10^{-16}
$B_3\,\lambda_{233}$	3×10^{-5}	3×10^{-2}

Among all the $B_i\lambda$ combinations, $B_1\lambda_{123}$, $B_1\lambda_{132}$, $B_2\lambda_{232}$ and $B_3\lambda_{233}$ are most important because they can provide large amplitudes via tree level diagrams. The amplitude can be approximated by $\mathcal{M} \approx B_i\lambda(\tan\beta\sin\alpha - \cos\alpha)/\left(\sqrt{2}M_s^2\right)$, where α is the mixing angle between two CP-even neutral Higgs. Even though heavy sneutrino masses tend to suppress the amplitudes, they would relax the bounds on B_i and λ more significantly, hence are favorable. Moreover μ_0 should not be too small in order to make product of B_i and λ to be below the bounds from leptonic radiative decays, i.e. $|B_1^*\lambda_{132}|$, $|B_1\lambda_{123}^*|$, $|B_2^*\lambda_{232}|$ and $|B_3\lambda_{233}^*| \lessapprox 1.4 \times 10^{-3}\,|\mu_0|^2$ [21]. It is noteworthy that even under stringent neutrino mass $\lesssim$ 1eV constraint, the four combinations could give branching ratios beyond 10^{-5}, which is large enough to be possibly probed at LHC. As to other $B_i\lambda$ combinations, they can be from several diagrams. However, they only play minor roles and hardly give any meaningful branching ratio, as shown in Table 3.

If we do not impose sub-eV neutrino mass bounds, $B_1\lambda_{123}$, $B_1\lambda_{132}$ and $B_2\lambda_{232}$ still get constrained by B_iB_i neutrino mass loops, while $B_3\lambda_{233}$ is not only constrained by B_iB_i

neutrino mass loops, but also limited by our manual "1% of B_0" bound. Comparing with neutrino mass $\lesssim$ 1eV case, branching ratios from B_2 and B_3 increase significantly while that from B_1 just raise a bit.

As a matter of fact, the class of $B_i\lambda$ combinations gives the most important contributions to the flavor violating Higgs decays among all RPV parameter combinations. Moreover, the approximation of tree level amplitudes as above could apply to $h^0 \to e\bar{\tau}+\tau\bar{e}$ and $h^0 \to e\bar{\mu}+\mu\bar{e}$ as well. As a result, under the same parameter setting, it is expected for $h^0 \to e\bar{\tau} + \tau\bar{e}$ and $h^0 \to e\bar{\mu} + \mu\bar{e}$ to give branching ratios with roughly the same order of magnitude as in $h^0 \to \mu\bar{\tau} + \tau\bar{\mu}$. However, it is pointed out [33] that LFV effective coupling between light Higgs, electron and muon could not be large because of the constraint set by two-loop Barr-Zee diagrams [34] on $\mu \to e\gamma$. Therefore, only $h^0 \to e\bar{\tau} + \tau\bar{e}$ is expected to give branching ratio comparable to which of $h^0 \to \mu\bar{\tau} + \tau\bar{\mu}$.

D. Contribution from $B_i\, A^\lambda$ combinations

Under our parameterization, A^λ's do not contribute to radiative decays such as $b \to s\gamma$ in one-loop level [21]. Therefore, A^λ's do not have known experimental constraints and, naively, can take any value. But the B_i parameters are limited by loop neutrino masses as before. Contributions from B_iA^λ may be quite interesting since this will be like first experimental signature of the RPV A-parameters. However, an A^λ only plays its role in the Higgs decay through Type2No.4 diagram with a neutral scalar-charged scalar-charged scalar ($h^0\phi^+\phi^-$) coupling. It is then expected to give a larger contribution at low charged scalar mass.

Table 4. $B_i\, A^\lambda$ contributions to branching ratio of $h^0 \to \mu\bar{\tau} + \tau\bar{\mu}$

RPV Parameter Combinations	With Neutrino Mass $\lesssim$1eV Constraint	With Relaxed Neutrino Mass Constraint
$B_1\, A^\lambda_{123}$	5×10^{-11}	2×10^{-10}
$B_1\, A^\lambda_{132}$	5×10^{-11}	2×10^{-10}
$B_2\, A^\lambda_{232}$	5×10^{-11}	7×10^{-7}
$B_3\, A^\lambda_{233}$	5×10^{-11}	1×10^{-7}

In our parameter setting, branching ratios from B_iA^λ combinations can reach order of 10^{-7} at most as shown in Table 4. However, if we allow A^λ to be as large as 3.1TeV (or

higher), order of 10^{-6} or above is possible. Since decay rate is proportional to amplitude square and hence A^λ square, it is easy to see how branching ratio modifies as A^λ increases [22].

E. Contribution from $\mu_i\,\lambda$ combinations

All $\mu_i\,\lambda$ combinations which can contribute to $h^0 \to \mu\bar{\tau}+\tau\bar{\mu}$ at one-loop level except $\mu_1\lambda_{123}$ and $\mu_1\lambda_{132}$, are constrained by their loop contributions to neutrino masses [31]. Again, single μ_i is constrained by its contribution to tree level neutrino mass. Leptonic radiative decays also give upper bounds on $\mu_i\,\lambda$, i.e. $|\mu_2^*\lambda_{232}|\,, |\mu_1^*\lambda_{132}|\,, |\mu_3\lambda_{233}^*|$ and $|\mu_1\lambda_{123}^*| \lessapprox 7.0\times10^{-4}\,|\mu_0|$ [21]. Further bounds for single λ by charged current experiments can be found in [32].

Table 5. $\mu_i\,\lambda$ contributions to branching ratio of $h^0 \to \mu\bar{\tau}+\tau\bar{\mu}$

RPV Parameter Combinations	With Neutrino Mass $\lesssim$1eV Constraint	With Relaxed Neutrino Mass Constraint
$\mu_1\,\lambda_{123}$	5×10^{-8}	5×10^{-8}
$\mu_1\,\lambda_{132}$	5×10^{-8}	5×10^{-8}
$\mu_2\,\lambda_{232}$	3×10^{-12}	5×10^{-8}
$\mu_2\,\lambda_{131}$	2×10^{-24}	2×10^{-16}
$\mu_3\,\lambda_{233}$	1×10^{-14}	5×10^{-8}
$\mu_3\,\lambda_{121}$	1×10^{-24}	5×10^{-19}

Many diagrams contribute to $h^0 \to \mu\bar{\tau}+\tau\bar{\mu}$ process via $\mu_i\,\lambda$ combinations. Among which, Type1No.3 and Type1No.4 diagrams play the most important roles. The requirement of neutrino mass $\lesssim$ 1eV still set most stringent bounds as in the case of other type combinations. However, $\mu_1\lambda_{123}$ and $\mu_1\lambda_{132}$ do not give loop contribution to neutrino masses, and thus they are mainly bounded by the constraints from radiative leptonic decays. Generally speaking, large slepton masses are favorable in order to have larger branching ratios since they can relax the constraints from loop neutrino masses and raise the upper bounds on the λ's.

In the condition that the neutrino masses being larger than 1eV, the leptonic decays become the major sources of constraints except for the case of $\mu_2\,\lambda_{131}$ and $\mu_3\,\lambda_{121}$. In any case, branching ratios from $\mu_i\,\lambda$ can only achieve at most the order of 10^{-8} in our analysis because of the stringent constraints from leptonic decays. Our results are shown in Table 5.

F. Contribution from the other insignificant combinations

In addition to the above combinations, there are some other types of combination (i.e., $B_i\,\lambda'$, $\mu_i\,\mu_j$, $\mu_i\,\lambda'$, $\lambda\,\lambda$ and $\lambda'\,\lambda'$) which can merely give negligible contributions. Hence we only list the combinations which are most illustrative or give the largest branching ratios in each type of combinations, as shown in Table 6. Note that the types of combination which are not mentioned, $\lambda''\,\lambda''$ for example, give zero contributions at one-loop level.

Table 6. The most interesting examples in the other RPV combinations

RPV Parameter Combinations	With Neutrino Mass $\lesssim$1eV Constraint	With Relaxed Neutrino Mass Constraint
$B_2\,\lambda'_{333}$	1×10^{-14}	2×10^{-11}
$B_3\,\lambda'_{233}$	1×10^{-15}	8×10^{-13}
$\mu_2\,\mu_3$	2×10^{-18}	2×10^{-18}
$\mu_2\,\lambda'_{323}$	3×10^{-18}	9×10^{-13}
$\mu_3\,\lambda'_{223}$	5×10^{-19}	5×10^{-14}
$\lambda_{232}\,\lambda_{233}$	2×10^{-19}	2×10^{-11}
$\lambda_{121}\,\lambda_{131}$	1×10^{-15}	1×10^{-15}
$\lambda_{123}\,\lambda_{133}$	2×10^{-10}	
$\lambda'_{211}\,\lambda'_{311}$	7×10^{-18}	9×10^{-16}
$\lambda'_{222}\,\lambda'_{322}$	4×10^{-22}	3×10^{-15}
$\lambda'_{223}\,\lambda'_{323}$	4×10^{-12}	
$\lambda'_{233}\,\lambda'_{333}$	5×10^{-26}	1×10^{-15}

In the $B_i\,\lambda'$ combinations, besides the constraints mentioned before on B_i, λ' also gets constrained by charged/neutral current experiments [32, 35]. $B_i\lambda'$ combinations contribute to $h^0\to\mu\bar{\tau}+\tau\bar{\mu}$ mainly via No.1 and No.2 diagrams of Type 6 and 7 (in Appendix A). To get better branching ratios, it is advantageous if we raise the upper bounds on B_i by the heavy sneutrino and neutralino masses. Heavy squark masses could also raise the upper bounds on λ'. However, in our computation, contributions from $B_i\lambda'$ can not provide sizable branching ratios.

As to $\mu_i\mu_j$ combinations, only $\mu_2\,\mu_3$ contributes to $h^0\to\mu\bar{\tau}+\tau\bar{\mu}$ up to the one-loop level. With non-zero μ_i, one of the neutrinos get tree level mass. However, leptonic radiative

decays set more stringent bound on $\mu_2\mu_3$ than neutrino mass does, i.e. $|\mu_2^*\mu_3| \lessapprox 3.6 \times 10^{-3}\,|\mu_0|^2$ [21]. Interestingly enough, though $\mu_2\mu_3$ combination contributes to the decay in tree level, loop contribution from Type1No.4 diagram is generally more important due to the smallness of neutrino masses in the loop. At any rate, $\mu_2\mu_3$ could only give a negligible branching ratio.

Among all $\mu_i\lambda'$'s which give non-zero contributions, some combinations are constrained by their loop contributions to neutrino masses [31]. Besides, every $\mu_i\,\lambda'$ is bounded by tree level neutrino mass constraints on μ_i and experimental constraints on single λ' [32, 35]. In this type of combinations, there is no obvious dominant diagram. Several diagrams can give comparable major contributions to $h^0 \to \mu\bar{\tau} + \tau\bar{\mu}$ process. Generally speaking, heavy gaugino masses can relax the tree level neutrino mass constraints while heavy down-squark masses can raise the upper bounds of λ' and relax loop neutrino mass constraints, hence they are favorable for larger branching ratios. Unfortunately, in whole parameter space, it is hard for the $\mu_i\lambda'$ to give any significant branching ratios, even in relaxed neutrino mass constraints.

Contributions from $\lambda\,\lambda$ combinations are mainly from No.3 and No.4 diagrams of Type 2, 6, and 7. Among all $\lambda\,\lambda$ combinations which contribute to $h^0 \to \mu\bar{\tau} + \tau\bar{\mu}$, only $\lambda_{232}\lambda_{233}$ and $\lambda_{121}\lambda_{131}$ are constrained by their loop contributions to neutrino masses [31]. However, leptonic decays could also provide upper bounds for $\lambda\lambda$ combinations [21, 32, 36]. Specifically, neutrino mass constraint on $\lambda_{121}\,\lambda_{131}$ contains a factor of electron mass, and hence is relaxed by the smallness of electron mass. Therefore the branching ratio from $\lambda_{121}\,\lambda_{131}$ is mainly limited by restriction from leptonic decays. On the other hand, neutrino mass constraint on $\lambda_{232}\,\lambda_{233}$ is enhanced by a τ mass factor. The later gives major restriction on branching ratio from $\lambda_{232}\,\lambda_{233}$ under the condition of neutrino mass $\lesssim$ 1eV. The best branching ratio from $\lambda\,\lambda$ we can have is of the order 10^{-10} at most.

Many diagrams can contribute to the Higgs decay via $\lambda'\,\lambda'$ combinations. Among which, Type1No.2 and Type2No.1 diagrams are most important ones. Just like the $\lambda\,\lambda$ case, among all $\lambda'\lambda'$ combinations which contribute to $h^0 \to \mu\bar{\tau} + \tau\bar{\mu}$, only $\lambda'_{211}\lambda'_{311}$, $\lambda'_{222}\lambda'_{322}$ and $\lambda'_{233}\lambda'_{333}$ as listed contribute to neutrino masses [31] and hence get additional constraints. Besides, radiative B decays and leptonic decays also give upper bounds on $\lambda'\,\lambda'$ [32, 36–38]. Particularly, under the neutrino mass $\lesssim$1eV condition, constraints on $\lambda'_{211}\lambda'_{311}$, $\lambda'_{222}\lambda'_{322}$ and $\lambda'_{233}\lambda'_{333}$ are suppressed/enhanced separately by the electron, muon, and tau mass factors.

This makes the differences between their branching ratios. However, if we allow neutrino masses being larger than 1eV, they will constrained by leptonic decays before exceeding experimental neutrino mass bounds. Nevertheless, $\lambda'\,\lambda'$ type of combinations could only give negligible contributions to $h^0 \to \mu\bar{\tau} + \tau\bar{\mu}$.

IV. SUMMARY

We have analyzed thoroughly Higgs to $\mu\bar{\tau} + \tau\bar{\mu}$ decay under the framework of minimal supersymmetric standard model without R parity. By means of full one-loop diagrammatic calculations and taking the RPV terms as the only source of lepton flavor violation, we showed that the branching ratio of $h^0 \to \mu\bar{\tau} + \tau\bar{\mu}$ could exceed 10^{-5} without contradicting experimental constraints. If indirect sub-eV neutrino mass bound is lifted, branching ratio of 10^{-2} is possible. We pull together the most interesting RPV parameter combinations and corresponding branching ratios in Table 7 for easy reference. Moreover, $h^0 \to e\bar{\tau} + \tau\bar{e}$ is expected to be able to give roughly the same order of branching ratio with that of $h^0 \to \mu\bar{\tau} + \tau\bar{\mu}$ from RPV terms, while $h^0 \to e\bar{\mu} + \mu\bar{e}$ is suppressed due to stringent constraint from two-loop Barr-Zee diagrams.

Table 7. Interesting contributions to branching ratio of $h^0 \to \mu\bar{\tau} + \tau\bar{\mu}$

RPV Parameter Combinations	With Neutrino Mass $\lesssim$1eV Constraint	With Relaxed Neutrino Mass Constraint
$B_2\,\mu_3$	1×10^{-15}	9×10^{-6}
$B_3\,\mu_2$	1×10^{-13}	7×10^{-4}
$B_1\,\lambda_{123}$	1×10^{-5}	4×10^{-5}
$B_1\,\lambda_{132}$	3×10^{-5}	7×10^{-5}
$B_2\,\lambda_{232}$	3×10^{-5}	6×10^{-2}
$B_3\,\lambda_{233}$	3×10^{-5}	3×10^{-2}
$B_2\,A^{\lambda}_{232}$	5×10^{-11}	7×10^{-7}
$B_3\,A^{\lambda}_{233}$	5×10^{-11}	1×10^{-7}

From an experimental point of view, a typical cross section of the MSSM 125 GeV Higgs at 8 TeV energy is of the order 10pb. For $Br(h^0 \to \mu\bar{\tau} + \tau\bar{\mu}) \gtrsim 10^{-5}$ and with a luminosity of the order 10 fb^{-1}, this would lead to several raw $\mu\bar{\tau} + \tau\bar{\mu}$ events with almost no SM

background. If we allow more free parameters or a larger parameter space during our analysis, the branching ratios can become even larger. Together with the 14 TeV energy for future LHC runs, we may have more events and a better chance to probe lepton flavor violation, and physics beyond the Standard Model.

Acknowledgements

Y.C. and O.K. are partially supported by research grant NSC 99- 2112-M-008-003-MY3 of the National Science Council of Taiwan.

Appendix A: One-Loop Feynman Diagrams in MSSM without R Parity for Neutral Higgs $\phi^0 \to \mu\bar{\tau}$

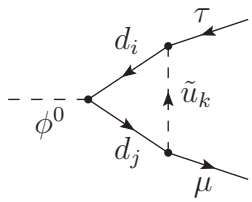

Type1No.1

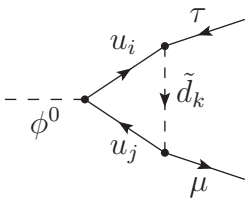

Type1No.2

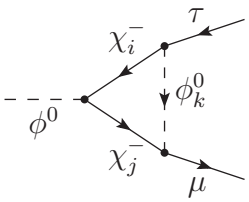

Type1No.3

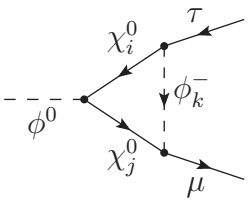

Type1No.4

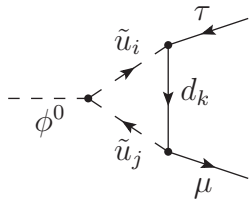

Type2No.1

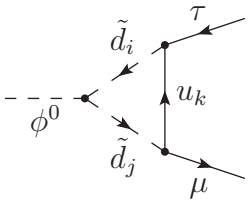

Type2No.2

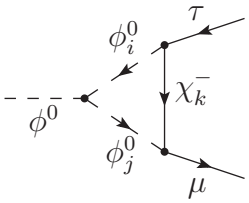

Type2No.3

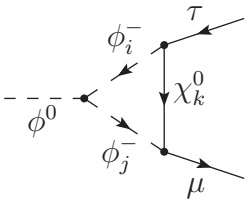

Type2No.4

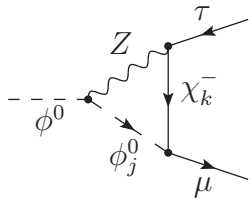

Type3No.1

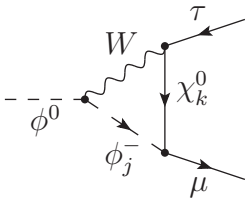

Type3No.2

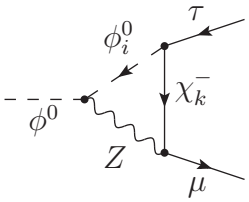

Type3No.3

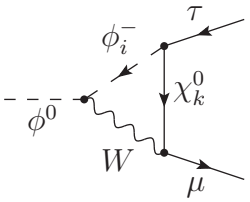

Type3No.4

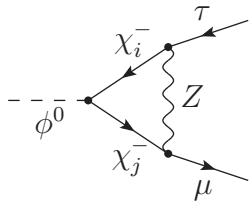

Type4No.1

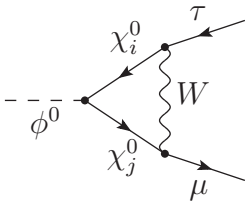

Type4No.2

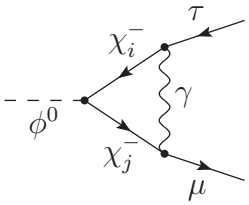

Type4No.3

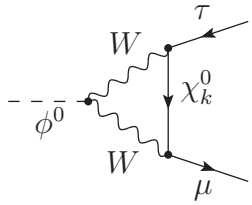

Type5No.1

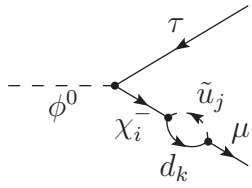

Type6No.1

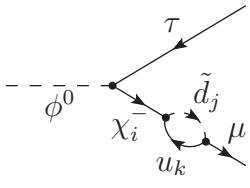

Type6No.2

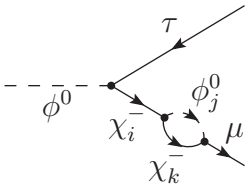

Type6No.3

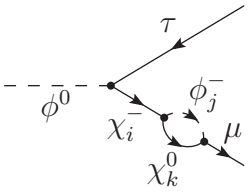

Type6No.4

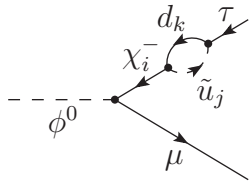

Type7No.1

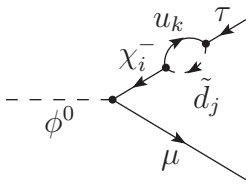

Type7No.2

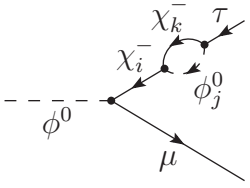

Type7No.3

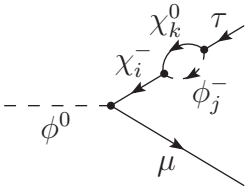

Type7No.4

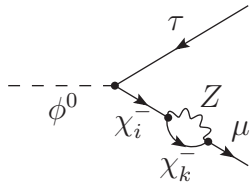

Type8No.1

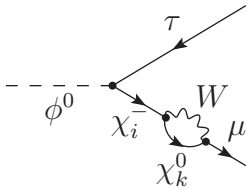

Type8No.2

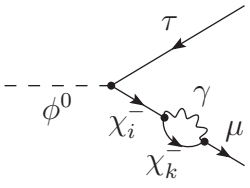

Type8No.3

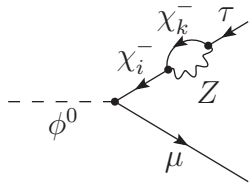

Type9No.1

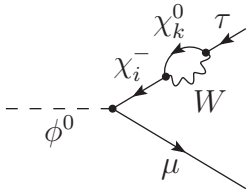

Type9No.2

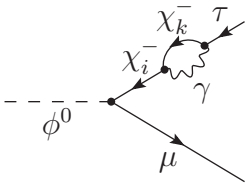

Type9No.3

Appendix B: Effective Couplings in MSSM without R Parity

We list all relevant effective mass eigenstate couplings for our analysis here. Indices run from 1 to 10 for neutral scalars (sleptons), 1 to 8 for charged scalars (sleptons), 1 to 6 for squarks, 1 to 7 for neutral fermions (neutralinos) and 1 to 5 for charged fermions (charginos) while all dummy indices run from 1 to 3. Moreover,

$$y_{u_i} = \frac{g_2 m_{u_i}}{\sqrt{2} M_W \sin\beta}\,, \quad y_{d_i} = \frac{g_2 m_{d_i}}{\sqrt{2} M_W \cos\beta}\,, \quad \text{and} \quad y_{e_i} = \frac{g_2 m_i}{\sqrt{2} M_W \cos\beta}$$

are the diagonal quark and charged lepton Yukawa couplings, where m_i's ($\approx m_{e_i}$ under small-μ_i scenario) are mass parameters in charged fermion mass matrix [23].

Neutral Scalar (Sneutrino)-W^+-W^- Vertices

$$\mathcal{L} = g^W_m W^+ W^- \phi^0_m$$

where

$$g^W_m = g_2 M_W \left(\sin\beta\, \mathcal{D}^s_{1m} + \cos\beta\, \mathcal{D}^s_{2m}\right) . \tag{B1}$$

Neutral Scalar-Chagred Scalar (Slepton)-W Vertices

$$\mathcal{L} = \mathcal{G}^W_{mn} \left[p(\phi^-_n) - p(\phi^0_m)\right]_\mu W^+ \phi^-_n \phi^0_m + \text{h.c.}$$

where

$$\mathcal{G}^W_{mn} = \frac{1}{2} g_2 \left[\left(\mathcal{D}^s_{1m} - i\mathcal{D}^s_{6m}\right)\mathcal{D}^l_{1n} - \left(\mathcal{D}^s_{2m} - i\mathcal{D}^s_{7m}\right)\mathcal{D}^l_{2n} - \left(\mathcal{D}^s_{(p+2)m} - i\mathcal{D}^s_{(p+7)m}\right)\mathcal{D}^l_{(p+2)n}\right] . \tag{B2}$$

Neutral Scalar-Neutral Scalar-Z Vertices

$$\mathcal{L} = \mathcal{G}^Z_{ij} \left[p(\phi^0_j) - p(\phi^0_i)\right]_\mu Z \phi^0_i \phi^0_j$$

where

$$\mathcal{G}^Z_{ij} = \frac{i}{2} g_Z \left(\mathcal{D}^s_{6i}\mathcal{D}^s_{1j} - \mathcal{D}^s_{1i}\mathcal{D}^s_{6j} + \mathcal{D}^s_{7i}\mathcal{D}^s_{2j} - \mathcal{D}^s_{2i}\mathcal{D}^s_{7j} + \mathcal{D}^s_{(q+7)i}\mathcal{D}^s_{(q+2)j} - \mathcal{D}^s_{(q+2)i}\mathcal{D}^s_{(q+7)j}\right) . \tag{B3}$$

Neutral Lepton (Neutralino)-Charged Lepton (Chargino)-W Vertices

$$\mathcal{L} = g_2 \overline{\Psi}(\chi^0_m)\Phi^\dagger(W^-) \left[\mathcal{N}^{wL}_{mi}\gamma_\mu \frac{1-\gamma_5}{2} + \mathcal{N}^{wR}_{mi}\gamma_\mu \frac{1+\gamma_5}{2}\right] \Psi(\chi^-_i) + \text{h.c.}$$

where

$$\mathcal{N}^{wL}_{mi} = -\boldsymbol{X}^*_{2m}\boldsymbol{U}_{1i} - \frac{1}{\sqrt{2}}\boldsymbol{X}^*_{4m}\boldsymbol{U}_{2i} - \frac{1}{\sqrt{2}}\boldsymbol{X}^*_{(q+4)m}\boldsymbol{U}_{(q+2)i}$$
$$\mathcal{N}^{wR}_{mi} = \boldsymbol{V}_{1i}\boldsymbol{X}_{2m} + \frac{1}{\sqrt{2}}\boldsymbol{V}_{2i}\boldsymbol{X}^*_{3m}\,. \tag{B4}$$

Charged Lepton-Charged Lepton-Z Vertices

$$\mathcal{L} = g_Z\overline{\Psi}(\chi^-_i)\left[\mathcal{C}^{zL}_{ij}\gamma_\mu\frac{1-\gamma_5}{2} + \mathcal{C}^{zR}_{ij}\gamma_\mu\frac{1+\gamma_5}{2}\right]\Phi(Z)\Psi(\chi^-_j)$$

where

$$\mathcal{C}^{zL}_{ij} = -\left(-1+\sin^2\theta_W\right)\boldsymbol{U}^*_{1i}\boldsymbol{U}_{1j} - \left(-\frac{1}{2}+\sin^2\theta_W\right)\boldsymbol{U}^*_{2i}\boldsymbol{U}_{2j} - \left(-\frac{1}{2}+\sin^2\theta_W\right)\boldsymbol{U}^*_{(q+2)i}\boldsymbol{U}_{(q+2)j}$$
$$\mathcal{C}^{zR}_{ij} = \left(1-\sin^2\theta_W\right)\boldsymbol{V}_{1j}\boldsymbol{V}^*_{1i} + \left(\frac{1}{2}-\sin^2\theta_W\right)\boldsymbol{V}_{2j}\boldsymbol{V}^*_{2i} - \sin^2\theta_W\boldsymbol{V}_{(q+2)j}\boldsymbol{V}^*_{(q+2)i}\,. \tag{B5}$$

Charged Lepton-Charged Lepton-γ Vertices

$$\mathcal{L} = e\overline{\Psi}(\chi^-_i)\left[\mathcal{C}^{\gamma L}_{ij}\gamma_\mu\frac{1-\gamma_5}{2} + \mathcal{C}^{\gamma R}_{ij}\gamma_\mu\frac{1+\gamma_5}{2}\right]\Phi(A^\mu)\Psi(\chi^-_j)$$

where

$$\mathcal{C}^{\gamma L}_{ij} = \boldsymbol{U}^*_{1i}\boldsymbol{U}_{1j} + \boldsymbol{U}^*_{2i}\boldsymbol{U}_{2j} + \boldsymbol{U}^*_{(q+2)i}\boldsymbol{U}_{(q+2)j}$$
$$\mathcal{C}^{\gamma R}_{ij} = \boldsymbol{V}_{1j}\boldsymbol{V}^*_{1i} + \boldsymbol{V}_{2j}\boldsymbol{V}^*_{2i} + \boldsymbol{V}_{(q+2)j}\boldsymbol{V}^*_{(q+2)i}\,. \tag{B6}$$

Charged Lepton-Down Quark-Up Squark Vertices

$$\mathcal{L}^{\chi^-} = g_2\overline{\Psi}(\chi^-_n)\Phi^\dagger(\tilde{u}_m)\left[\mathcal{C}^{dL}_{nmi}\frac{1-\gamma_5}{2} + \mathcal{C}^{dR}_{nmi}\frac{1+\gamma_5}{2}\right]\Psi(d_i) + \text{h.c.}$$

where

$$\mathcal{C}^{dL}_{nmi} = -\boldsymbol{V}^*_{1n}\mathcal{D}^{u*}_{im} + \frac{y_{u_j}}{g_2}V^{ji}_{CKM}\boldsymbol{V}^*_{2n}\mathcal{D}^{u*}_{(j+3)m}$$
$$\mathcal{C}^{dR}_{nmi} = \frac{y_{d_i}}{g_2}\boldsymbol{U}^*_{2n}\mathcal{D}^{u*}_{im} + \frac{\lambda'^*_{jhi}}{g_2}\boldsymbol{U}^*_{(j+2)n}\mathcal{D}^{u*}_{hm}\,. \tag{B7}$$

Neutral Scalar-Quark-Quark Vertices: Down Sector

$$\mathcal{L}^{\phi^0} = g_2\overline{\Psi}(d_h)\Phi^\dagger(\phi^0_m)\left[\widetilde{\mathcal{N}}^{dL}_{hmi}\frac{1-\gamma_5}{2} + \widetilde{\mathcal{N}}^{dR}_{hmi}\frac{1+\gamma_5}{2}\right]\Psi(d_i)$$

where

$$\widetilde{\mathcal{N}}^{dL}_{hmi} = -\frac{y_{d_i}}{\sqrt{2}g_2}\delta_{ih}\left(\mathcal{D}^s_{2m} + i\mathcal{D}^s_{7m}\right) - \frac{\lambda'_{kih}}{\sqrt{2}g_2}\left(\mathcal{D}^s_{(k+2)m} + i\mathcal{D}^s_{(k+7)m}\right)$$
$$\widetilde{\mathcal{N}}^{dR}_{hmi} = -\frac{y_{d_i}}{\sqrt{2}g_2}\delta_{ih}\left(\mathcal{D}^s_{2m} - i\mathcal{D}^s_{7m}\right) - \frac{\lambda'^*_{khi}}{\sqrt{2}g_2}\left(\mathcal{D}^s_{(k+2)m} - i\mathcal{D}^s_{(k+7)m}\right) . \tag{B8}$$

Neutral Scalar-Quark-Quark Vertices: Up Sector

$$\mathcal{L}^u = g_2\overline{\Psi}(u_h)\Phi^\dagger(\phi^0_m)\left[\widetilde{\mathcal{N}}^{uL}_{hmi}\frac{1-\gamma_5}{2} + \widetilde{\mathcal{N}}^{uR}_{hmi}\frac{1+\gamma_5}{2}\right]\Psi(u_i)$$

where

$$\widetilde{\mathcal{N}}^{uL}_{hmi} = -\frac{y_{u_i}}{\sqrt{2}g_2}\delta_{ih}\left(\mathcal{D}^s_{1m} - i\mathcal{D}^s_{6m}\right)$$
$$\widetilde{\mathcal{N}}^{uR}_{hmi} = -\frac{y_{u_i}}{\sqrt{2}g_2}\delta_{ih}\left(\mathcal{D}^s_{1m} + i\mathcal{D}^s_{6m}\right) . \tag{B9}$$

Charged Lepton-Up Quark-Down Squark Vertices

$$\mathcal{L}^{\chi^+} = g_2\overline{\Psi}(\chi^+_n)\Phi^\dagger(\tilde{d}_m)\left[\mathcal{C}^{uL}_{nmi}\frac{1-\gamma_5}{2} + \mathcal{C}^{uR}_{nmi}\frac{1+\gamma_5}{2}\right]\Psi(u_i) + \text{h.c.}$$

where

$$\mathcal{C}^{uL}_{nmi} = -V^{ip*}_{CKM}\boldsymbol{U}_{1n}\mathcal{D}^{d*}_{pm} + \frac{y_{d_p}}{g_2}V^{ip*}_{CKM}\boldsymbol{U}_{2n}\mathcal{D}^{d*}_{(p+3)m} + \frac{\lambda'_{jhp}}{g_2}V^{ih*}_{CKM}\boldsymbol{U}_{(j+2)n}\mathcal{D}^{d*}_{(p+3)m}$$
$$\mathcal{C}^{uR}_{nmi} = \frac{y_{u_i}}{g_2}V^{ip*}_{CKM}\boldsymbol{V}_{2n}\mathcal{D}^{d*}_{pm} . \tag{B10}$$

Neutral Scalar-Charged Lepton-Charged Lepton Vertices

$$\mathcal{L} = g_2\overline{\Psi}(\chi^-_{\bar{n}})\left[\mathcal{C}^{\chi L}_{\bar{n}mn}\frac{1-\gamma_5}{2} + \mathcal{C}^{\chi R}_{\bar{n}mn}\frac{1+\gamma_5}{2}\right]\Psi(\chi^-_n)\Phi(\phi^0_m)$$

where

$$\begin{aligned}
\mathcal{C}^{\chi L}_{\bar{n}mn} =& -\frac{1}{\sqrt{2}}\boldsymbol{V}^*_{2\bar{n}}\boldsymbol{U}_{1n}(\mathcal{D}^s_{1m}+i\mathcal{D}^s_{6m}) - \frac{1}{\sqrt{2}}\boldsymbol{V}^*_{1\bar{n}}\boldsymbol{U}_{2n}(\mathcal{D}^s_{2m}-i\mathcal{D}^s_{7m}) \\
&- \frac{1}{\sqrt{2}}\boldsymbol{V}^*_{1\bar{n}}\boldsymbol{U}_{(j+2)n}(\mathcal{D}^s_{(j+2)m}-i\mathcal{D}^s_{(j+7)m}) - \frac{y_{e_j}}{\sqrt{2}g_2}\boldsymbol{V}^*_{(j+2)\bar{n}}\boldsymbol{U}_{(j+2)n}(\mathcal{D}^s_{2m}+i\mathcal{D}^s_{7m}) \\
&+ \frac{y_{e_j}}{\sqrt{2}g_2}\boldsymbol{V}^*_{(j+2)\bar{n}}\boldsymbol{U}_{2n}(\mathcal{D}^s_{(j+2)m}+i\mathcal{D}^s_{(j+7)m}) + \frac{\lambda_{ijk}}{\sqrt{2}g_2}\boldsymbol{V}^*_{(k+2)\bar{n}}\boldsymbol{U}_{(i+2)n}(\mathcal{D}^s_{(j+2)m}+i\mathcal{D}^s_{(j+7)m}) \\
\mathcal{C}^{\chi R}_{\bar{n}mn} =& -\frac{1}{\sqrt{2}}\boldsymbol{U}^*_{1\bar{n}}\boldsymbol{V}_{2n}(\mathcal{D}^s_{1m}-i\mathcal{D}^s_{6m}) - \frac{1}{\sqrt{2}}\boldsymbol{U}^*_{2\bar{n}}\boldsymbol{V}_{1n}(\mathcal{D}^s_{2m}+i\mathcal{D}^s_{7m}) \\
&- \frac{1}{\sqrt{2}}\boldsymbol{U}^*_{(j+2)\bar{n}}\boldsymbol{V}_{1n}(\mathcal{D}^s_{(j+2)m}+i\mathcal{D}^s_{(j+7)m}) - \frac{y_{e_j}}{\sqrt{2}g_2}\boldsymbol{U}^*_{(j+2)\bar{n}}\boldsymbol{V}_{(j+2)n}(\mathcal{D}^s_{2m}-i\mathcal{D}^s_{7m}) \\
&+ \frac{y_{e_j}}{\sqrt{2}g_2}\boldsymbol{U}^*_{2\bar{n}}\boldsymbol{V}_{(j+2)n}(\mathcal{D}^s_{(j+2)m}-i\mathcal{D}^s_{(j+7)m}) \\
&+ \frac{\lambda^*_{ijk}}{\sqrt{2}g_2}\boldsymbol{U}^*_{(i+2)\bar{n}}\boldsymbol{V}_{(k+2)n}(\mathcal{D}^s_{(j+2)m}-i\mathcal{D}^s_{(j+7)m})\,. \qquad \text{(B11)}
\end{aligned}$$

Neutral Scalar-Neutral Lepton-Neutral Lepton Vertices

$$\mathcal{L} = g_2\overline{\Psi}(\chi^0_{\bar{n}})\left[\mathcal{N}^{\chi L}_{\bar{n}mn}\frac{1-\gamma_5}{2} + \mathcal{N}^{\chi R}_{\bar{n}mn}\frac{1+\gamma_5}{2}\right]\Psi(\chi^0_n)\Phi(\phi^0_m)$$

where

$$\begin{aligned}
\mathcal{N}^{\chi L}_{\bar{n}mn} =& \quad \frac{1}{2}\left(-\tan\theta_W\boldsymbol{X}_{1\bar{n}} + \boldsymbol{X}_{2\bar{n}}\right)\boldsymbol{X}^*_{3n}(\mathcal{D}^s_{1m}+i\mathcal{D}^s_{6m}) \\
&+ \frac{1}{2}\left(\tan\theta_W\boldsymbol{X}_{1\bar{n}} - \boldsymbol{X}_{2\bar{n}}\right)\boldsymbol{X}_{4n}(\mathcal{D}^s_{2m}-i\mathcal{D}^s_{7m}) \\
&+ \frac{1}{2}\left(\tan\theta_W\boldsymbol{X}_{1\bar{n}} - \boldsymbol{X}_{2\bar{n}}\right)\boldsymbol{X}_{(k+4)n}(\mathcal{D}^s_{(k+2)m}-i\mathcal{D}^s_{(k+7)m}) \\
\mathcal{N}^{\chi R}_{\bar{n}mn} =& \quad \frac{1}{2}\boldsymbol{X}_{3\bar{n}}\left(-\tan\theta_W\boldsymbol{X}^*_{1n} + \boldsymbol{X}^*_{2n}\right)(\mathcal{D}^s_{1m}-i\mathcal{D}^s_{6m}) \\
&+ \frac{1}{2}\boldsymbol{X}^*_{4\bar{n}}\left(\tan\theta_W\boldsymbol{X}^*_{1n} - \boldsymbol{X}^*_{2n}\right)(\mathcal{D}^s_{2m}+i\mathcal{D}^s_{7m}) \\
&+ \frac{1}{2}\boldsymbol{X}^*_{(k+4)\bar{n}}\left(\tan\theta_W\boldsymbol{X}^*_{1n} - \boldsymbol{X}^*_{2n}\right)(\mathcal{D}^s_{(k+2)m}+i\mathcal{D}^s_{(k+7)m})\,. \qquad \text{(B12)}
\end{aligned}$$

Charged Scalar-Neutral Lepton-Charged Lepton Vertices

$$\mathcal{L} = g_2\overline{\Psi}(\chi^-_{\bar{n}})\left[\widetilde{\mathcal{C}}^{\chi L}_{\bar{n}mn}\frac{1-\gamma_5}{2} + \widetilde{\mathcal{C}}^{\chi R}_{\bar{n}mn}\frac{1+\gamma_5}{2}\right]\Psi(\chi^0_n)\Phi(\phi^-_m) + \text{h.c.}$$

where

$$\begin{aligned}
\widetilde{\mathcal{C}}^{\chi L}_{\bar{n}mn} =& -\boldsymbol{V}^*_{1\bar{n}}\boldsymbol{X}^*_{3n}\mathcal{D}^l_{1m} + \frac{\sqrt{2}}{2}\boldsymbol{V}^*_{2\bar{n}}\left(-\tan\theta_W\boldsymbol{X}_{1n} - \boldsymbol{X}_{2n}\right)\mathcal{D}^l_{1m} \\
&- \sqrt{2}\tan\theta_W\boldsymbol{V}^*_{(j+2)\bar{n}}\boldsymbol{X}_{1n}\mathcal{D}^l_{(j+5)m} - \frac{y_{e_j}}{g_2}\left(\boldsymbol{V}^*_{(j+2)\bar{n}}\boldsymbol{X}_{4n}\mathcal{D}^l_{(j+2)m} - \boldsymbol{V}^*_{(j+2)\bar{n}}\boldsymbol{X}_{(j+4)n}\mathcal{D}^l_{2m}\right) \\
&- \frac{\lambda_{ijk}}{g_2}\boldsymbol{V}^*_{(k+2)\bar{n}}\boldsymbol{X}_{(i+4)n}\mathcal{D}^l_{(j+2)m} \\
\widetilde{\mathcal{C}}^{\chi R}_{\bar{n}mn} =& -\boldsymbol{U}^*_{1\bar{n}}\boldsymbol{X}^*_{4n}\mathcal{D}^l_{2m} - \boldsymbol{U}^*_{1\bar{n}}\boldsymbol{X}^*_{(k+4)n}\mathcal{D}^l_{(k+2)m} + \frac{\sqrt{2}}{2}\boldsymbol{U}^*_{2\bar{n}}\left(\tan\theta_W\boldsymbol{X}^*_{1n} + \boldsymbol{X}^*_{2n}\right)\mathcal{D}^l_{2m} \\
&+ \frac{\sqrt{2}}{2}\boldsymbol{U}^*_{(k+2)\bar{n}}\left(\tan\theta_W\boldsymbol{X}^*_{1n} + \boldsymbol{X}^*_{2n}\right)\mathcal{D}^l_{(k+2)m} \\
&- \frac{y_{e_k}}{g_2}\left(\boldsymbol{U}^*_{(k+2)\bar{n}}\boldsymbol{X}^*_{4n}\mathcal{D}^l_{(k+5)m} - \boldsymbol{U}^*_{2\bar{n}}\boldsymbol{X}^*_{(k+4)n}\mathcal{D}^l_{(k+5)m}\right) \\
&- \frac{\lambda^*_{ijk}}{g_2}\boldsymbol{U}^*_{(j+2)\bar{n}}\boldsymbol{X}^*_{(i+4)n}\mathcal{D}^l_{(k+5)m}\,. \qquad \text{(B13)}
\end{aligned}$$

Neutral Scalar-Squark-Squark Vertices: Down-Sector

$$\mathcal{L} = \boldsymbol{g}^d_{abm}\,\Phi^\dagger(\tilde{d}_a)\Phi(\tilde{d}_b)\Phi(\phi^0_m)$$

where

$$\begin{aligned}
\boldsymbol{g}^d_{abm} =& \frac{g_2 M_Z}{\cos\theta_W}\left(\frac{1}{2} - \frac{1}{3}\sin^2\theta_W\right)\left(\cos\beta\,\mathcal{D}^s_{2m} - \sin\beta\,\mathcal{D}^s_{1m}\right)\mathcal{D}^{d*}_{qa}\mathcal{D}^d_{qb} \\
&+ \frac{g_2 M_Z}{\cos\theta_W}\left(\frac{1}{3}\sin^2\theta_W\right)\left(\cos\beta\,\mathcal{D}^s_{2m} - \sin\beta\,\mathcal{D}^s_{1m}\right)\mathcal{D}^{d*}_{(q+3)a}\mathcal{D}^d_{(q+3)b} \\
&- \sqrt{2}\,y_{d_q}\,m_{d_q}\mathcal{D}^{d*}_{qa}\mathcal{D}^d_{qb}\mathcal{D}^s_{2m} - \sqrt{2}\,y_{d_q}\,m_{d_q}\mathcal{D}^{d*}_{(q+3)a}\mathcal{D}^d_{(q+3)b}\mathcal{D}^s_{2m} \\
&+ \frac{1}{\sqrt{2}}\left(\mu^*_0\,\delta_{pq}\,y_{d_q} + \mu^*_i\lambda^{'}_{ipq}\right)\mathcal{D}^{d*}_{(q+3)a}\mathcal{D}^d_{pb}\left(\mathcal{D}^s_{1m} + i\mathcal{D}^s_{6m}\right) \\
&+ \frac{1}{\sqrt{2}}\left(\mu_0\,\delta_{pq}\,y_{d_q} + \mu_i\lambda^{'*}_{ipq}\right)\mathcal{D}^{d*}_{pa}\mathcal{D}^d_{(q+3)b}\left(\mathcal{D}^s_{1m} - i\mathcal{D}^s_{6m}\right) \\
&- \frac{1}{\sqrt{2}}A^D_{pq}\mathcal{D}^{d*}_{(q+3)a}\mathcal{D}^d_{pb}\left(\mathcal{D}^s_{2m} + i\mathcal{D}^s_{7m}\right) - \frac{1}{\sqrt{2}}A^{D*}_{pq}\mathcal{D}^{d*}_{pa}\mathcal{D}^d_{(q+3)b}\left(\mathcal{D}^s_{2m} - i\mathcal{D}^s_{7m}\right) \\
&- \frac{1}{\sqrt{2}}A^{\lambda'}_{jpq}\mathcal{D}^{d*}_{(q+3)a}\mathcal{D}^d_{pb}\left(\mathcal{D}^s_{(j+2)m} + i\mathcal{D}^s_{(j+7)m}\right) \\
&- \frac{1}{\sqrt{2}}A^{\lambda'*}_{jpq}\mathcal{D}^{d*}_{pa}\mathcal{D}^d_{(q+3)b}\left(\mathcal{D}^s_{(j+2)m} - i\mathcal{D}^s_{(j+7)m}\right) \\
&- \frac{1}{\sqrt{2}}\left[m_{d_p}\lambda^{'}_{ipq}\mathcal{D}^d_{(p+3)b}\mathcal{D}^{d*}_{(q+3)a} + m_{d_q}\lambda^{'}_{ipq}\mathcal{D}^{d*}_{qa}\mathcal{D}^d_{pb}\right]\left(\mathcal{D}^s_{(i+2)m} + i\mathcal{D}^s_{(i+7)m}\right) \\
&- \frac{1}{\sqrt{2}}\left[m_{d_p}\lambda^{'*}_{ipq}\mathcal{D}^{d*}_{(p+3)a}\mathcal{D}^d_{(q+3)b} + m_{d_q}\lambda^{'*}_{ipq}\mathcal{D}^d_{qb}\mathcal{D}^{d*}_{pa}\right]\left(\mathcal{D}^s_{(i+2)m} - i\mathcal{D}^s_{(i+7)m}\right)\,. \qquad \text{(B14)}
\end{aligned}$$

Neutral Scalar-Squark-Squark Vertices: Up-Sector

$$\mathcal{L} = \boldsymbol{g}^{u}_{abm}\, \Phi^{\dagger}(\tilde{u}_a)\Phi(\tilde{u}_b)\Phi(\phi^0_m)$$

where

$$\begin{aligned}
\boldsymbol{g}^{u}_{abm} =& \frac{g_2 M_Z}{\cos\theta_W}\left(-\frac{1}{2}+\frac{2}{3}\sin^2\theta_W\right)\left(\cos\beta\,\mathcal{D}^{s}_{2m}-\sin\beta\,\mathcal{D}^{s}_{1m}\right)\mathcal{D}^{u*}_{qa}\mathcal{D}^{u}_{qb} \\
&-\frac{g_2 M_Z}{\cos\theta_W}\left(\frac{2}{3}\sin^2\theta_W\right)\left(\cos\beta\,\mathcal{D}^{s}_{2m}-\sin\beta\,\mathcal{D}^{s}_{1m}\right)\mathcal{D}^{u*}_{(q+3)a}\mathcal{D}^{u}_{(q+3)b} \\
&-\sqrt{2}\,y_{u_l} m_{u_l} V^{lp*}_{CKM} V^{lq}_{CKM}\mathcal{D}^{u*}_{pa}\mathcal{D}^{u}_{qb}\mathcal{D}^{s}_{1m} - \sqrt{2}\,y_{u_q} m_{u_q}\mathcal{D}^{u*}_{(q+3)a}\mathcal{D}^{u}_{(q+3)b}\mathcal{D}^{s}_{1m} \\
&+\frac{1}{\sqrt{2}} y_{u_q} V^{qp}_{CKM}\left[\mu^*_0\left(\mathcal{D}^{s}_{2m}-i\mathcal{D}^{s}_{7m}\right)+\mu^*_j\left(\mathcal{D}^{s}_{(j+2)m}-i\mathcal{D}^{s}_{(j+7)m}\right)\right]\mathcal{D}^{u*}_{(q+3)a}\mathcal{D}^{u}_{pb} \\
&+\frac{1}{\sqrt{2}} y_{u_q} V^{qp*}_{CKM}\left[\mu_0\left(\mathcal{D}^{s}_{2m}+i\mathcal{D}^{s}_{7m}\right)+\mu_j\left(\mathcal{D}^{s}_{(j+2)m}+i\mathcal{D}^{s}_{(j+7)m}\right)\right]\mathcal{D}^{u*}_{pa}\mathcal{D}^{u}_{(q+3)b} \\
&-\frac{1}{\sqrt{2}} A^{U}_{pq}\mathcal{D}^{u*}_{(q+3)a}\mathcal{D}^{u}_{pb}\left(\mathcal{D}^{s}_{1m}-i\mathcal{D}^{s}_{6m}\right) \\
&-\frac{1}{\sqrt{2}} A^{U*}_{pq}\mathcal{D}^{u*}_{pa}\mathcal{D}^{u}_{(q+3)b}\left(\mathcal{D}^{s}_{1m}+i\mathcal{D}^{s}_{6m}\right)\,. \qquad \text{(B15)}
\end{aligned}$$

Cubic Neutral Scalar Vertices

$$\mathcal{L} = \boldsymbol{g}^{0}_{abm}\Phi(\phi^0_a)\Phi(\phi^0_b)\Phi(\phi^0_m)$$

where

$$\begin{aligned}
\boldsymbol{g}^{0}_{abm} =& \frac{g_2 M_Z}{4\cos\theta_W}\left(\cos\beta\mathcal{D}^{s}_{2m}-\sin\beta\mathcal{D}^{s}_{1m}\right)\times \\
&\left(\mathcal{D}^{s}_{1a}\mathcal{D}^{s}_{1b}+\mathcal{D}^{s}_{6a}\mathcal{D}^{s}_{6b}-\mathcal{D}^{s}_{2a}\mathcal{D}^{s}_{2b}-\mathcal{D}^{s}_{7a}\mathcal{D}^{s}_{7b}-\mathcal{D}^{s}_{(q+2)a}\mathcal{D}^{s}_{(q+2)b}-\mathcal{D}^{s}_{(q+7)a}\mathcal{D}^{s}_{(q+7)b}\right) \\
&+\text{permutations in } (a,b,m)\,. \qquad \text{(B16)}
\end{aligned}$$

Neutral Scalar-Charged Scalar-Charged Scalar Vertices

$$\mathcal{L} = \boldsymbol{g}^{-}_{abm}\Phi^{\dagger}(\phi^{-}_{a})\Phi(\phi^{-}_{b})\Phi(\phi^{0}_{m})$$

where

$$\begin{aligned}
\boldsymbol{g}^{-}_{abm} = &-\frac{1}{2}\frac{g_2 M_Z}{\cos\theta_W}\sin\beta\,\mathcal{D}^{s}_{1m}\mathcal{D}^{l*}_{1a}\mathcal{D}^{l}_{1b} + \frac{g_2 M_Z}{\cos\theta_W}\left(-\frac{1}{2}+\sin^2\theta_W\right)\cos\beta\,\mathcal{D}^{s}_{2m}\mathcal{D}^{l*}_{1a}\mathcal{D}^{l}_{1b}\\
&-\frac{1}{2}\frac{g_2 M_Z}{\cos\theta_W}\left(1-\sin^2\theta_W\right)\left[\cos\beta\,\left(\mathcal{D}^{s}_{1m}-i\mathcal{D}^{s}_{6m}\right)+\sin\beta\,\left(\mathcal{D}^{s}_{2m}+i\mathcal{D}^{s}_{7m}\right)\right]\mathcal{D}^{l*}_{2a}\mathcal{D}^{l}_{1b}\\
&-\frac{1}{2}\frac{g_2 M_Z}{\cos\theta_W}\left(1-\sin^2\theta_W\right)\left[\cos\beta\,\left(\mathcal{D}^{s}_{1m}+i\mathcal{D}^{s}_{6m}\right)+\sin\beta\,\left(\mathcal{D}^{s}_{2m}-i\mathcal{D}^{s}_{7m}\right)\right]\mathcal{D}^{l*}_{1a}\mathcal{D}^{l}_{2b}\\
&-\frac{1}{2}\frac{g_2 M_Z}{\cos\theta_W}\left(1-\sin^2\theta_W\right)\left(\sin\beta\,\mathcal{D}^{l}_{1b}+\cos\beta\,\mathcal{D}^{l}_{2b}\right)\left(\mathcal{D}^{s}_{(i+2)m}+i\mathcal{D}^{s}_{(i+7)m}\right)\mathcal{D}^{l*}_{(q+2)a}\\
&-\frac{1}{2}\frac{g_2 M_Z}{\cos\theta_W}\left(1-\sin^2\theta_W\right)\left(\sin\beta\,\mathcal{D}^{l*}_{1a}+\cos\beta\,\mathcal{D}^{l*}_{2a}\right)\left(\mathcal{D}^{s}_{(i+2)m}-i\mathcal{D}^{s}_{(i+7)m}\right)\mathcal{D}^{l}_{(q+2)b}\\
&-\frac{1}{2}\frac{g_2 M_Z}{\cos\theta_W}\cos\beta\,\mathcal{D}^{s}_{2m}\mathcal{D}^{l*}_{2a}\mathcal{D}^{l}_{2b} - \frac{g_2 M_Z}{\cos\theta_W}\left(\frac{1}{2}-\sin^2\theta_W\right)\sin\beta\,\mathcal{D}^{s}_{1m}\mathcal{D}^{l*}_{2a}\mathcal{D}^{l}_{2b}\\
&+\frac{g_2 M_Z}{\cos\theta_W}\left(\frac{1}{2}-\sin^2\theta_W\right)\left(\cos\beta\,\mathcal{D}^{s}_{2m}-\sin\beta\,\mathcal{D}^{s}_{1m}\right)\mathcal{D}^{l*}_{(q+2)a}\mathcal{D}^{l}_{(q+2)b}\\
&+\frac{g_2 M_Z}{\cos\theta_W}\left(\sin^2\theta_W\right)\left(\cos\beta\,\mathcal{D}^{s}_{2m}-\sin\beta\,\mathcal{D}^{s}_{1m}\right)\mathcal{D}^{l*}_{(q+5)a}\mathcal{D}^{l}_{(q+5)b}\\
&-\sqrt{2}\,y_{e_q}m_{e_q}\mathcal{D}^{l*}_{(q+2)a}\mathcal{D}^{l}_{(q+2)b}\mathcal{D}^{s}_{2m} - \sqrt{2}\,y_{e_q}m_{e_q}\mathcal{D}^{l*}_{(q+5)a}\mathcal{D}^{l}_{(q+5)b}\mathcal{D}^{s}_{2m}\\
&-\frac{1}{\sqrt{2}}\mu^{*}_{q}y_{e_q}\mathcal{D}^{l*}_{(q+5)a}\mathcal{D}^{l}_{2b}\left(\mathcal{D}^{s}_{1m}+i\mathcal{D}^{s}_{6m}\right) - \frac{1}{\sqrt{2}}\mu_{q}y_{e_q}\mathcal{D}^{l*}_{2a}\mathcal{D}^{l}_{(q+5)b}\left(\mathcal{D}^{s}_{1m}-i\mathcal{D}^{s}_{6m}\right)\\
&-\frac{1}{\sqrt{2}}\mu^{*}_{q}y_{e_q}\mathcal{D}^{l*}_{(q+5)a}\mathcal{D}^{l}_{1b}\left(\mathcal{D}^{s}_{2m}+i\mathcal{D}^{s}_{7m}\right) - \frac{1}{\sqrt{2}}\mu_{q}y_{e_q}\mathcal{D}^{l*}_{1a}\mathcal{D}^{l}_{(q+5)b}\left(\mathcal{D}^{s}_{2m}-i\mathcal{D}^{s}_{7m}\right)\\
&+\frac{1}{\sqrt{2}}\left(\mu^{*}_{0}\delta_{pq}y_{e_q}+\mu^{*}_{i}\lambda_{ipq}\right)\mathcal{D}^{l*}_{(q+5)a}\mathcal{D}^{l}_{(p+2)b}\left(\mathcal{D}^{s}_{1m}+i\mathcal{D}^{s}_{6m}\right)\\
&+\frac{1}{\sqrt{2}}\left(\mu_{0}\delta_{pq}y_{e_q}+\mu_{i}\lambda^{*}_{ipq}\right)\mathcal{D}^{l*}_{(p+2)a}\mathcal{D}^{l}_{(q+5)b}\left(\mathcal{D}^{s}_{1m}-i\mathcal{D}^{s}_{6m}\right)\\
&+\frac{1}{\sqrt{2}}\left(\mu^{*}_{0}\delta_{pq}y_{e_q}+\mu^{*}_{i}\lambda_{ipq}\right)\mathcal{D}^{l*}_{(q+5)a}\mathcal{D}^{l}_{1b}\left(\mathcal{D}^{s}_{(p+2)m}+i\mathcal{D}^{s}_{(p+7)m}\right)\\
&+\frac{1}{\sqrt{2}}\left(\mu_{0}\delta_{pq}y_{e_q}+\mu_{i}\lambda^{*}_{ipq}\right)\mathcal{D}^{l*}_{1a}\mathcal{D}^{l}_{(q+5)b}\left(\mathcal{D}^{s}_{(p+2)m}-i\mathcal{D}^{s}_{(p+7)m}\right)\\
&+\frac{1}{\sqrt{2}}m_{e_q}y_{e_q}\mathcal{D}^{l*}_{(q+2)a}\mathcal{D}^{l}_{2b}\left(\mathcal{D}^{s}_{(q+2)m}+i\mathcal{D}^{s}_{(q+7)m}\right)\\
&+\frac{1}{\sqrt{2}}m_{e_q}y_{e_q}\mathcal{D}^{l*}_{2a}\mathcal{D}^{l}_{(q+2)b}\left(\mathcal{D}^{s}_{(q+2)m}-i\mathcal{D}^{s}_{(q+7)m}\right)
\end{aligned}$$

$$
\begin{aligned}
&- \frac{1}{\sqrt{2}} m_{e_p} \lambda_{jpq} \mathcal{D}^{l*}_{(q+5)a} \mathcal{D}^{l}_{(p+5)b} \left(\mathcal{D}^{s}_{(j+2)m} + i \mathcal{D}^{s}_{(j+7)m} \right) \\
&- \frac{1}{\sqrt{2}} m_{e_p} \lambda^{*}_{jpq} \mathcal{D}^{l*}_{(p+5)a} \mathcal{D}^{l}_{(q+5)b} \left(\mathcal{D}^{s}_{(j+2)m} - i \mathcal{D}^{s}_{(j+7)m} \right) \\
&- \frac{1}{\sqrt{2}} m_{e_q} \lambda_{jpq} \mathcal{D}^{l*}_{(q+2)a} \mathcal{D}^{l}_{(p+2)b} \left(\mathcal{D}^{s}_{(j+2)m} + i \mathcal{D}^{s}_{(j+7)m} \right) \\
&- \frac{1}{\sqrt{2}} m_{e_q} \lambda^{*}_{jpq} \mathcal{D}^{l*}_{(p+2)a} \mathcal{D}^{l}_{(q+2)b} \left(\mathcal{D}^{s}_{(j+2)m} - i \mathcal{D}^{s}_{(j+7)m} \right) \\
&- \frac{1}{\sqrt{2}} A^{E}_{pq} \mathcal{D}^{l*}_{(q+5)a} \mathcal{D}^{l}_{(p+2)b} \left(\mathcal{D}^{s}_{2m} + i \mathcal{D}^{s}_{7m} \right) - \frac{1}{\sqrt{2}} A^{E*}_{pq} \mathcal{D}^{l*}_{(p+2)a} \mathcal{D}^{l}_{(q+5)b} \left(\mathcal{D}^{s}_{2m} - i \mathcal{D}^{s}_{7m} \right) \\
&+ \frac{1}{\sqrt{2}} A^{E}_{pq} \mathcal{D}^{l*}_{(q+5)a} \mathcal{D}^{l}_{2b} \left(\mathcal{D}^{s}_{(p+2)m} + i \mathcal{D}^{s}_{(p+7)m} \right) + \frac{1}{\sqrt{2}} A^{E*}_{pq} \mathcal{D}^{l*}_{2a} \mathcal{D}^{l}_{(q+5)b} \left(\mathcal{D}^{s}_{(p+2)m} - i \mathcal{D}^{s}_{(p+7)m} \right) \\
&- \frac{1}{\sqrt{2}} A^{\lambda}_{jpq} \mathcal{D}^{l*}_{(q+5)a} \mathcal{D}^{l}_{(p+2)b} \left(\mathcal{D}^{s}_{(j+2)m} + i \mathcal{D}^{s}_{(j+7)m} \right) \\
&- \frac{1}{\sqrt{2}} A^{\lambda*}_{jpq} \mathcal{D}^{l*}_{(p+2)a} \mathcal{D}^{l}_{(q+5)b} \left(\mathcal{D}^{s}_{(j+2)m} - i \mathcal{D}^{s}_{(j+7)m} \right) \ . \qquad \text{(B17)}
\end{aligned}
$$

---

[1] S. Fukuda *et al.* [Super-Kamiokande Collaboration], Phys. Rev. Lett. **85**, 3999 (2000) [arXiv:hep-ex/0009001].

[2] M. H. Ahn *et al.* [K2K Collaboration], Phys. Rev. D **74**, 072003 (2006) [arXiv:hep-ex/0606032].

[3] Q. R. Ahmad *et al.* [SNO Collaboration], Phys. Rev. Lett. **87**, 071301 (2001) [arXiv:nucl-ex/0106015].

[4] K. Eguchi, *et al.* [KamLAND Collaboration], Phys. Rev. Lett. **90**, 021802 (2003) [arXiv:hep-ex/0212021].

[5] F. Borzumati and A. Masiero, Phys. Rev. Lett. **57**, 961 (1986); J. Hisano, T. Moroi, K. Tobe, M. Yamaguchi, and T. Yanagida, Phys. Lett. B **357**, 579 (1995) [arXiv:hep-ph/9501407]; J. Hisano, T. Moroi, K. Tobe, and M. Yamaguchi, Phys. Rev. D **53**, 2442 (1996) [arXiv:hep-ph/9510309]; J. Hisano and D. Nomura, Phys. Rev. D **59**, 116005 (1999) [arXiv:hep-ph/9810479]; E. Arganda, A. M. Curiel, M. J. Herrero, and D. Temes, Phys. Rev. D **71**, 035011 (2005) [arXiv:hep-ph/0407302]; K. S. Babu and C. Kolda, Phys. Rev. Lett. **89**, 241802 (2002) [arXiv:hep-ph/0206310]; J. K. Parry, Nucl. Phys. B **760**, 38 (2007) [arXiv:hep-ph/0510305].

[6] T. P. Cheng and M. Sher, Phys. Rev. D **35**, 3484 (1987); T. Han and D. Marfatia, Phys. Rev. Lett. **86**, 1442 (2001) [arXiv:hep-ph/0008141].

[7] S. Kanemura, K. Matsuda, T. Ota, T. Shindou, E. Takasugi, and K. Tsumura, Phys. Lett. B **599**, 83 (2004) [arXiv:hep-ph/0406316].

[8] S. Chatrchyan *et al.* [CMS Collaboration], Phys. Rev. Lett. **107**, 221804 (2011) [arXiv:1109.2352 [hep-ex]]; G. Aad *et al.* [ATLAS Collaboration], Phys. Rev. D **85**, 112006 (2012) [arXiv:1203.6193 [hep-ex]]; G. Aad *et al.* [ATLAS Collaboration], Phys. Rev. Lett. **108**, 241802 (2012) [arXiv:1203.5763 [hep-ex]].

[9] C. Strege, G. Bertone, D. G. Cerdeno, M. Fornasa, R. Ruiz de Austri, and R. Trotta, JCAP **03**, 030 (2012) [arXiv:1112.4192 [hep-ph]]; O. Buchmueller, R. Cavanaugh, A. De Roeck, M. J. Dolan, J. R. Ellis, H. Flacher, S. Heinemeyer, G. Isidori, D. M. Santos, K. A. Olive, S. Rogerson, F. J. Ronga, and G. Weiglein, Eur. Phys. J. C **72**, 1878 (2012) [arXiv:1110.3568 [hep-ph]].

[10] S. Akula, N. Chen, D. Feldman, M. Liu, Z. Liu, P. Nath, and G. Peim, Phys. Lett. B **699**, 377 (2011) [arXiv:1103.1197 [hep-ph]].

[11] S. S. AbdusSalam, Phys. Lett. B **705**, 331 (2011) [arXiv:1106.2317 [hep-ph]]; A. Arbey, M. Battaglia, and F. Mahmoudi, Eur. Phys. J. C **72**, 1847 (2012) [arXiv:1110.3726 [hep-ph]]; S. Sekmen, S. Kraml, J. Lykken, F. Moortgat, S. Padhi, L. Pape, M. Pierini, H. B. Prosper, and M. Spiropulu, JHEP **1202**, 075 (2012) [arXiv:1109.5119 [hep-ph]].

[12] S. Akula, D. Feldman, Z. Liu, P. Nath, and G. Peim, Mod. Phys. Lett. A **26**, 1521 (2011) [arXiv:1103.5061 [hep-ph]]; S. Caron, J. Laamanen, I. Niessen, and A. Strübig, JHEP **1206**, 008 (2012) [arXiv:1202.5288 [hep-ph]].

[13] P. Bechtle, K. Desch, H. K. Dreiner, M. Kramer, B. O'Leary, C. Robens, B. Sarrazin, and P. Wienemann, Phys. Rev. D **84**, 011701 (2011) [arXiv:1102.4693 [hep-ph]].

[14] G. Aad *et al.* [ATLAS Collaboration], Phys. Lett. B **716**, 1 (2012) [arXiv:1207.7214 [hep-ex]].

[15] S. Chatrchyan *et al.* [CMS Collaboration], Phys. Lett. B **716**, 30 (2012) [arXiv:1207.7235 [hep-ex]].

[16] H. Baer, V. Barger, and A. Mustafayev, Phys. Rev. D **85**, 075010 (2012) [arXiv:1112.3017 [hep-ph]].

[17] M. Sher, Phys. Rev. D **66**, 057301 (2002) [arXiv:hep-ph/0207136]; A. Brignole and A. Rossi, Nucl. Phys. B **701**, 3 (2004) [arXiv:hep-ph/0404211]; D. A. Sierra, W. Porod, D. Restrepo

and C. E. Yaguna, Phys. Rev. D **78**, 015015 (2008) [arXiv:0804.1907 [hep-ph]].

[18] A. Brignole and A. Rossi, Phys. Lett. B **566**, 217 (2003) [arXiv:hep-ph/0304081].

[19] S. P. Martin, Phys. Rev. D **54**, 2340 (1996) [arXiv:hep-ph/9602349]; P. F. Pérez and S. Spinner, Phys. Lett. B **673**, 251 (2009) [arXiv:0811.3424 [hep-ph]].

[20] A. de Gouvêa, S. Lola, and K. Tobe, Phys. Rev. D **63**, 035004 (2001) [arXiv:hep-ph/0008085]; D. F. Carvalho, M. E. Gómez, and J. C. Romão, Phys. Rev. D **65**, 093013 (2002) [arXiv:hep-ph/0202054]; A. Gemintern, S. Bar-Shalom, G. Eilam, and F. Krauss, Phys. Rev. D **67**, 115012 (2003) [arXiv:hep-ph/0302186]; Y. -B. Sun, L. Han, W. -G. Ma, F. Tabbakh, R. -Y. Zhang, and Y. -J. Zhou, JHEP **0409**, 043 (2004) [arXiv:hep-ph/0409240]; R. Bose, J. Phys. G: Nucl. Part. Phys. **38**, 065003 (2011) [arXiv:1012.1736 [hep-ph]].

[21] K. Cheung and O. C. W. Kong, Phys. Rev. D **64**, 095007 (2001) [arXiv:hep-ph/0101347]; C. -Y. Chen and O. C. W. Kong, Phys. Rev. D **79**, 115013 (2009) [arXiv:0901.3371 [hep-ph]].

[22] A. Arhrib, Y. Cheng, and O. C. W. Kong, NCU-HEP-k053 [arXiv:1208.4669 [hep-ph]].

[23] O. C. W. Kong, Int. J. Mod. Phys. A **19**, 1863 (2004) [arXiv:hep-ph/0205205].

[24] M. Bisset, O. C. W. Kong, C. Macesanu, and L. H. Orr, Phys. Lett. B **430**, 274 (1998) [arXiv:hep-ph/9804282].

[25] M. Carena, J. Ellis, A. Pilaftsis, and C. E. M. Wagner, Nucl. Phys. B **586**, 92 (2000) [arXiv:hep-ph/0003180].

[26] S. Heinemeyer, W. Hollik, and G. Weiglein, Phys. Lett. B **455**, 179 (1999) [arXiv:hep-ph/9903404].

[27] T. Hahn, Nucl. Phys. Proc. Suppl. **89**, 231 (2000) [arXiv:hep-ph/0005029]; G. J. van Oldenborgh and J. A. M. Vermaseren, Z. Phys. **C46**, 425 (1990).

[28] S. P. Martin, In *Kane, G.L. (ed.): Perspectives on supersymmetry II* 1-153 [arXiv:hep-ph/9709356].

[29] D. N. Spergel *et al.* [WMAP Collaboration], Astrophys. J. Suppl. **148**, 175 (2003) [arXiv:astro-ph/0302209]; G. L. Fogli, E. Lisi, A. Marrone, and A. Palazzo, Prog. Part. Nucl. Phys. **57**, 742 (2006) [arXiv:hep-ph/0506083].

[30] S. Eidelman *et al.* [Particle Data Group], Phys. Lett. B **592**, 1 (2004).

[31] Y. Grossman and S. Rakshit, Phys. Rev. D **69**, 093002 (2004) [arXiv:hep-ph/0311310]; S. Rakshit, Mod. Phys. Lett. A **19**, 2239 (2004) [arXiv:hep-ph/0406168]; S. Davidson and M. Losada, Phys. Rev. D **65**, 075025 (2002) [arXiv:hep-ph/0010325].

[32] R. Barbier, C. Bérat, M. Besancon, M. Chemtob, A. Deandrea, E. Dudas, P. Fayet, S. Lavignac, G. Moreau, E. Perez, and Y. Sirois, Phys. Rept. **420**, 1 (2005) [arXiv:hep-ph/0406039].

[33] A. Goudelis, O. Lebedev, and J. -H. Park, Phys. Lett. B **707**, 369 (2012) [arXiv:1111.1715 [hep-ph]]; G. Blankenburg, J. Ellis, and G. Isidori, Phys. Lett. B **712**, 386 (2012) [arXiv:1202.5704 [hep-ph]]; R. Harnik, J. Kopp, and J. Zupan, [arXiv:1209.1397 [hep-ph]].

[34] S. M. Barr and A. Zee, Phys. Rev. Lett. **65**, 21 (1990) [Erratum-ibid. **65**, 2920 (1990)].

[35] G. Bhattacharyya, J. Ellis, and K. Sridhar, Mod. Phys. Lett. A **10**, 1583 (1995) [arXiv:hep-ph/9503264].

[36] H. K. Dreiner, M. Kramer, and B. O'Leary, Phys. Rev. D **75**, 114016 (2007) [arXiv:hep-ph/0612278].

[37] O. C. W. Kong and R. Vaidya, Phys. Rev. D **71**, 055003 (2005) [arXiv:hep-ph/0403148].

[38] J. P. Saha and A. Kundu, Phys. Rev. D **66**, 054021 (2002) [arXiv:hep-ph/0205046]; C. S. Kim and R. -M. Wang, Phys. Lett. B **681**, 44 (2009) [arXiv:0904.0318 [hep-ph]]; G. Bhattacharyya, K. B. Chatterjee, and S. Nandi, Nucl. Phys. B **831**, 344 (2010) [arXiv:0911.3811[hep-ph]].